Spanish pilot virtual tests report

Deliverable DB3.2

Real-time pollution-based control of urban drainage and sanitation systems for protection of receiving waters

Document Title : **LIFE RUBIES DB3.2.- Spanish pilot virtual tests report**	
Partner responsible : AQUATEC	
Authors : **AQUATEC, Cetaqua, CSIC, Canal de Isabel II**	Date: **December 2023**

Modifications (dates)
December 2023: Final and validated version

Table of contents

List of figures

List of tables

1 Introduction

This deliverable DB3.2 corresponds to the Action B.3 of LIFE RUBIES project called "Spanish Pilot site deployment operation" and specifically to the sub-action "B.3-3: Virtual testing". This sub-action focuses on adapting the Model-Predictive Control (MPC) controller considered in Madrid pilot site (LIFE RUBIES DB3.1 deliverable) to the characteristics of the network and test its performance considering real rain scenarios and using the Madrid pilot detailed sewer model as a virtual reality. In this sense, a software demonstrator has been developed in this sub-action in order to reproduce the real-time closed-loop interaction between the reality and the controller (Figure 1).

This software demonstrator allows to simulate a complete rain scenario computing the optimal set-points for the network actuators and applying them to the virtual reality. Once, the simulation ends, main KPIs as CSO volumes and Mass released to the environment can be computed. In this sense, the performance of the current operation (i.e. default control rules implemented in the hydraulic model provided by the operator) and the one computed by the MPC controller can be compared using a set of real rain scenarios in terms of resulting impacts on the receiving bodies (i.e. CSO volumes and Mass). These virtual tests allow to refine and validate the MPC controller as a previous stage to its real demonstration in the pilot site.

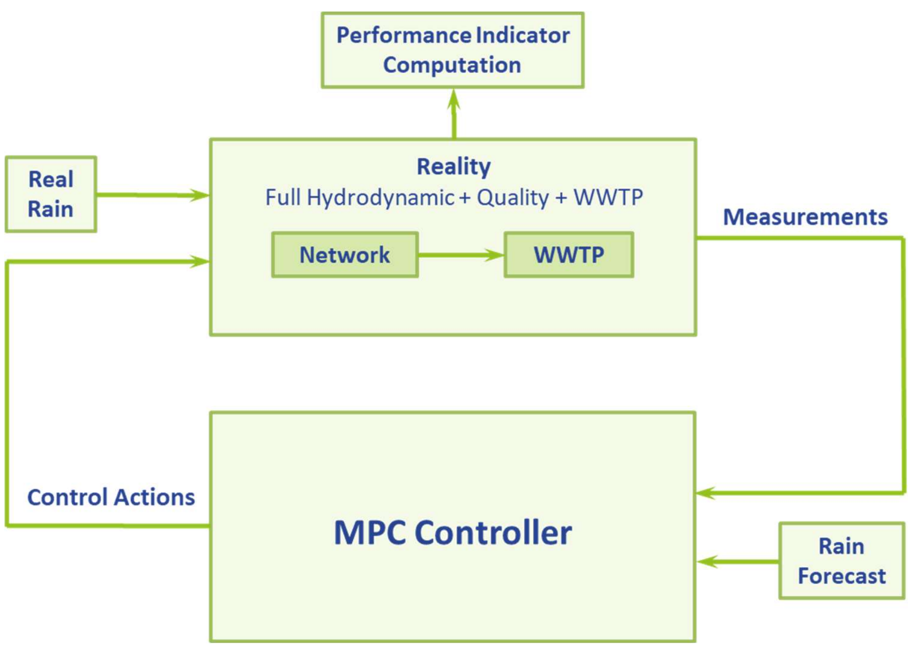

Figure 1 Real-time closed-loop between Reality (UDN+WWTP) and the controller

The remainder of this deliverable is structured as follows: in Chapter 2, the implemented software demonstrator is described, while the control methodology considered in the MPC controller is detailed in Chapter 3; regarding this methodology, the development of the needed simplified model associated with the Madrid pilot network is explained in Chapter 4; finally, in

Chapter 5, the results obtained comparing the MPC controller and the current operation performance considering real rain scenarios and using the software demonstrator is described. Finally, Chapter 6 provides the conclusions of the work developed as well as the next steps to be done

2 Software Demonstrator

As mentioned in Chapter 1, the software demonstrator allows to simulate the real-time interaction between the MPC controller and the (virtual) reality during a rain scenario. In this process, at every simulation time instant k (i.e. 5 minutes), the following loop is carried out: the current rain and the network states (i.e. tank levels) are read, then, the MPC controller computes optimal set-points for the actuators and they are applied to the virtual reality (network detailed model) running one-time step simulation. Then, the next loop corresponding to k+1 time instant can start.

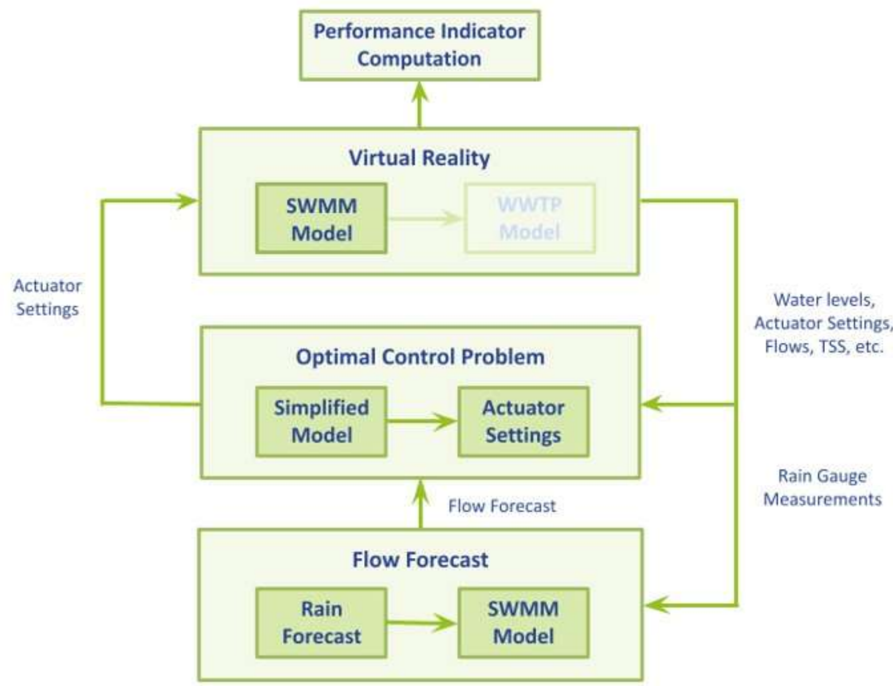

Figure 2 Real-time closed-loop between Reality (UDN) and the controller

Figure 2 depicts the detailed workflow considered in the implementation of the software demonstrator. Given the pilot network is just a small part of the complete Madrid system located at the downstream end, apart from the rain measurements, a forecast of the upstream flows entering the pilot area is needed. In this sense, the software demonstrator works with two SWMM instances implementing the Madrid sewer system model:

- A SWMM instance acting as a virtual reality, in which the network outside the pilot perimeter is operated according to the reference rules used by the operator and the pilot network is operated according to the set-points computed by the MPC controller at every time instant.
- A SWMM instance forecasting pilot network inflows from time instant k to time instant k+6 (i.e. 30-minutal prediction horizon considering 5-minutal time steps). In this sense, using the current rain at time instant k, the software demonstrator forecasts the rain

values for interval [k, k+6] and runs 30-minutal SWMM simulation to forecast pilot network inflows used for the MPC controller.

According to the closed-loop depicted in Figure 2, every time instant k (5 minutes):

- The current rain and the network states (i.e. tank levels, flows, TSS) are read.
- The pilot network inflows in the interval [k, k+6] are forecasted.
- The actuator set-points for the interval [k, k+6] are computed by the MPC controller.
- The computed set-points at time instant k are applied to the virtual reality running 1-time instant simulation from time instant k to k+1.

Once the full rain scenario is simulated, main KPIs related to the impacts on the environments as CSO volumes and released Mass can be computed.

This closed-loop can also be run by considering that actuators are operated according to the reference operation used by the operator. In this way, the performance of the MPC controller can be compared with the reference operation using a set of real scenarios.

To implement the workflow depicted in Figure 2, the software demonstrator has been implemented in Python in an object-oriented manner. A wrapper class called `MPC` contains all the necessary elements to run a closed-loop simulation including the controller parametrization (e.g., prediction horizon, time step), the SWMM model relevant elements for both simulation and forecast (tanks, nodes, links and actuators), the variable names of the simplified model implemented in GAMS (input and output), and the paths to the SWMM files and GAMS executable. The `MPC` object is initialized through a json file containing all the necessary information. The json file used in the simulations described in this document is as follows:

```
{
    "H": 6,
    "dt": 300,
    "inp_file": "Manzanares_v31_2_RainTS_NoControls.inp",
    "rain_file": "Arroyofresno_calib2_P0.txt",
    "hotstart_file": "Hotstart_24h_DWF_11.hsf",
    "gms_file": "Model.gms",
    "gams_exe": "C:/Program Files (x86)/GAMS23.9/gams.exe",
    "swmm_variables": {
        "tanks": [
            "Dip_Butarque",
            "Abronyigal"
        ],
        "nodes": "nodes.txt",
        "links": "links.txt",
        "actuators": [
            "NUD0059.5",
            "NUD0059.1",
            "NUD0059.2",
            "NUD0059.3",
            "NUD0059.4",
            "ALV0006.2",
            "ALV0002.1"
```

```
        ]
    },
    "gams_variables": {
        "input_variables": [
            "Qin1",
            "Qin2",
            "Qin3",
            "Qin4",
            "Qin5",
            "Qin6"
        ],
        "output_variables": [
            "Vaux",
            "Qaux1",
            "Qaux2",
            "Qmdaux",
            "Q12",
            "Qmd",
            "Qmd2",
            "Qmdmi",
            "Qmd3",
            "Q45",
            "Qcso1",
            "Q",
            "Qmarge",
            "Qcso2",
            "G",
            "Gin1",
            "Gout",
            "Gbuidat",
            "VButarque",
            "Gin2",
            "Q910",
            "QauxN10",
            "QauxN10_d1",
            "QauxN10_d2",
            "QauxN10_d3",
            "QcsoButarque",
            "QwwtpButarque",
            "QwwtpButarque1",
            "QwwtpButarque2",
            "GinA",
            "GoutA",
            "Gbuidat2",
            "VAbronyigal",
            "Qcso4",
            "Qmi",
            "P7",
            "Q1216",
            "Qmi2",
            "Qmdmi2",
            "Qcso5",
            "Qmi3",
            "QwwtpSur",
            "QcsoSur",
            "AuxP7"
```

```
        ],
        "objective_variables": [
            "dGin1",
            "dGout",
            "dGbuidat",
            "dGin2",
            "dGinA",
            "dGbuidat2",
            "JwwtpButarque",
            "JwwtpSur",
            "Jcso",
            "Jwwtp",
            "Jsmooth",
            "J"
        ]
    }
}
```


Two additional classes have also been implemented to manage the SWMM simulations and the GAMS optimization problems. The `SWMM` class subclasses the `PySWMM` class, freely available through the `pyswmm` Python module, and adds a few additional methods and attributes to run hydraulic simulations while easing the handling of rain time-series, initial and final simulation times, actuator setting modification and results extraction. Finally, the GAMS class implements the execution of the `gams.exe` file to solve the consecutive optimal control problems arising in MPC, the extraction of the solution of these problems, and the modification of the input and initial conditions files. Figure 3 shows the different `SWMM` and `GAMS` class instances appearing as attributes of an `MPC` class instance.

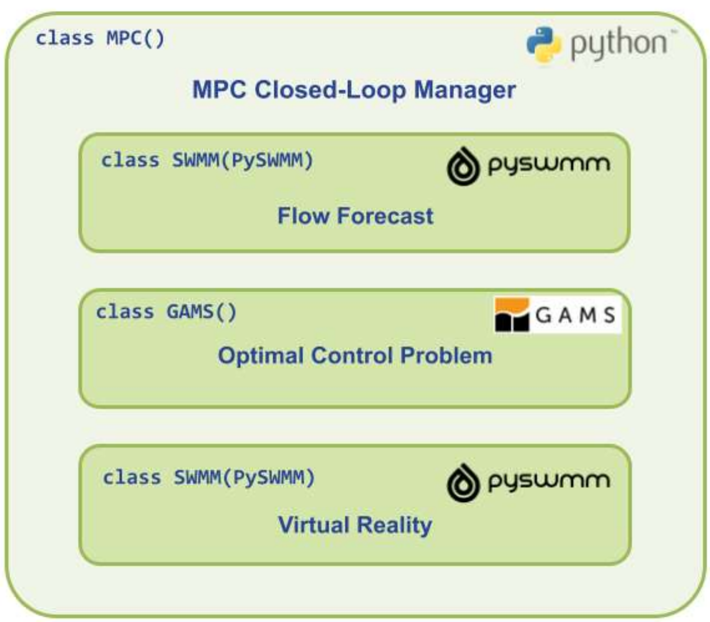

Figure 3 Main attributes of an MPC class instance to run MPC closed-loop simulations.

3 Control methodology applied to the Spanish pilot

As described in detail in deliverable DB1.1, in Madrid pilot, a Model-predictive control (MPC)-based controller is applied (MPC Controller). This controller is based on solving on-line finite-horizon optimal control problems formulated using the system mathematical model as constraints and last system measurements as model updates (Camacho and Bordons, 2004). In general, control objectives are formulated in terms of an objective function $\boldsymbol{J}$ to be minimized over a time ahead finite- horizon H to compute the optimal control law. In the MPC methodology, the optimal control problems are solved numerically on-line allowing for the inclusion of additional information to the problem such as constraints on the system variables (i.e., actuator bounds) or disturbance forecasts.

The general Optimal control problem (OCP) formulation addressed during the operation of the MPC controller at time-step t will be named OCP(t), and it follows the structure outlined in Equation (1). To distinguish the different problems and their corresponding solutions, the time instant in which these problems are formulated and solved is added to each variable. For example $\widehat{\boldsymbol{x}}(k|t)$ is the value of variable $\widehat{\boldsymbol{x}}$ at time-step k as computed (predicted) at time step t ≤ k solving the problem OCP(t) at time instant t.

$$\min_{\boldsymbol{X}(t),\boldsymbol{U}(t)} \boldsymbol{J}\big(\boldsymbol{X}(t), \boldsymbol{U}(t), \boldsymbol{W}(t)\big) \tag{1}$$

$$\begin{gathered}
\text{s.t.} \\
\widehat{\boldsymbol{x}}(t) = \boldsymbol{x_0} \\
\widehat{\boldsymbol{x}}(k+1|t) = \boldsymbol{g_1}\big(\widehat{\boldsymbol{x}}(k|t), \boldsymbol{u}(k|t), \boldsymbol{w}(k|t)\big), k = t, \dots, t+H-1 \\
\boldsymbol{g_2}\big(\hat{x}(k|t), \boldsymbol{u}(k|t), \boldsymbol{w}(k|t)\big) \le 0, k = t, \dots, t+H \\
\boldsymbol{x_{min}} \le \widehat{\boldsymbol{x}}(k|t) \le \boldsymbol{x_{max}}, k = t, \dots, t+H \\
\boldsymbol{u_{min}} \le \boldsymbol{u}(k|t) \le \boldsymbol{u_{max}}, k = t, \dots, t+H
\end{gathered}$$

where H is the time ahead optimization horizon; $\boldsymbol{g1}$ and $\boldsymbol{g2}$ determine the system model (i.e. simplified model); $\boldsymbol{x_0}$ is the initial values of the model states at time instant t obtained from the available system measurements (i.e. tank levels); $\boldsymbol{X}(t) = \big(\widehat{\boldsymbol{x}}(t|t), \widehat{\boldsymbol{x}}(t+1|t), \dots, \widehat{\boldsymbol{x}}(t+H|t)\big)$ is the sequence of the system states computed at time instant t (i.e. tank levels) ; $\boldsymbol{U}(t) = \big(\boldsymbol{u}(t|t), \boldsymbol{u}(t+1|t), \dots, \boldsymbol{u}(t+H|t)\big)$ is the sequence of the control actions computed at time instant t (gate positions, pumping flows); $\boldsymbol{W}(t) = \big(\boldsymbol{w}(t|t), \boldsymbol{w}(t+1|t), \dots, \boldsymbol{w}(t+H|t)\big)$ is the sequence of the disturbances as forecasted at time-step t (i.e. rain).

The objective function $\boldsymbol{J}(k)$ to be optimized is defined as a summation of different goals, which can be separated into hydraulic and quality objectives:

- Hydraulic objectives

The main objectives related to the network hydraulic behavior are the following:

- The minimization of the CSO discharges from the sewer network to the water receiving bodies, expressed as the sum (or squared sum) of the different CSO flows, i.e., $\boldsymbol{J_{CSO}}(k)$:

$$\boldsymbol{J_{CSO}}(k) = \sum_{i=1}^{n_{CSO}} q_{CSO}^{i}(k), \quad k = t, \dots, t+H$$

- The optimization of the WWTP operation, by sending the maximum allowed inlet flow. This value (or its square) is used as $\boldsymbol{J_{WWTP}}(k)$:

$$\boldsymbol{J_{WWTP}}(k) = \sum_{i=1}^{n_{WWTP}} \left(q_{WWTP}^{i}(k) - q_{lim}^{i} \quad\right)^2, \quad k = t, \dots, t+H$$

- The minimization of the excess of volumes/flows in tanks or sewers with respect to the operational safety values. This objective is computed as the sum (or squared sum) of the positive differences between actual and safety values, i.e., $\boldsymbol{J_{safety}}(k)$:

$$diff(k) = \max(0, x(k) - x_{max}), \quad k = t, \dots, t+H$$

$$\boldsymbol{J_{safety}}(k) = \sum_{i=1}^{n_{safety}} \left(diff^{i}(k)\right)^2, \quad k = t, \dots, t+H$$

- The maximization of the smoothness of the control actions through time, so that the differences between a certain control action value at a time step, and its value at the next one, are minimized. By summing these differences for all actuators and pairs of time instant-subsequent time instant, $\boldsymbol{J_{smooth}}(k)$ is obtained:

$$\boldsymbol{J_{smooth}}(k) = \sum_{i=1}^{n_{act}} \left(u^{i}(k) - u^{i}(k-1)\right)^2, \quad k = t+1, \dots, t+H$$

➢ Quality objectives

The main quality objective is related to the minimization of the CSO pollutants loads to the environment, expressed as the sum (or squared sum) of the different CSO masses, i.e., $\boldsymbol{J_{mass}}(k)$:

$$\boldsymbol{J_{mass}}(k) = \sum_{i=1}^{n_{CSO}} tss_{CSO}^{i}(k) q_{CSO}^{i}(k), \qquad k = t, \dots, t+H$$

Where $tss_{cso}^{i}(k)$ is the mass concentration associated with the CSO flow $q_{cso}^{i}(k)$ at the CSO point *i.*

Considering these goals, the objective function $J(k)$ can be written as follows:

$$J(k) = a_{mass}J_{mass}(k) + a_{cso}J_{cso}(k) + a_{wwtp}J_{wwtp}(k) + a_{safety}J_{safety}(k) + a_{smooth}J_{smooth}(k) \quad (2)$$

where the different goals are weighted according to their importance. For this problem, the safety goal has the highest priority to avoid flooding and damage to the infrastructures. Then, the CSO/mass and WWTP goals are prioritized to protect the environment and the treatment plant respectively. Finally, the smooth goal to guarantee the smoothness of the control actions protecting the existing actuators is considered.

For the virtual tests presented in this deliverable, given they are carried out off-line without connection to the real-time measurements of the mass concentration at the CSO points, the term $J_{mass}(k)$ is neglected. Thus, for the MPC Controller, all CSO points have the same consideration to release those water volumes that neither can be stored nor treated. However, for the envisaged on-line tests, this goal will be considered instead of $J_{cso}(k)$. In this case, at every time instant t, the OCP(t) problem is solved and the measurements of the mass concentrations $tss_{cso}^{i}(t)$ will be used to determine the priorities of the CSO points to release the CSO flows. At every time instant *t,* those CSO points having the lowest mass concentration will be the ones with highest priority to minimize the total mass released to the receiving body. These priorities may change according to the evolution over the time of the mass concentration at the CSO points.

As depicted in Eq. 1, the MPC methodology requires the mathematical equations associated with the hydrology and hydraulics involved in the urban drainage networks. However, due to the complexity of these processes, the use of detailed models in MPC-based RTC applications is not feasible. Consequently, simplified deterministic models are used instead, which can predict the approximate spatial and temporal evolution of the hydraulics and quality parameters. The development of the mathematical equations of the simplified model representing hydraulics and hydrology of the pilot network has been one of the crucial steps to apply the MPC methodology, as described in Chapter 4.

4 Development of the simplified model

4.1 Overview of the Madrid pilot and the network detailed model

As described in deliverable DA1.2, The pilot site is in the downstream part of the Manzanares system. The pilot site includes (Figure 4):

- 2 detention tanks: Butarque and Abroñigales tanks with a capacity of 359.000 m^3 and 200.000 m^3, respectively.
- 3 WWTPs: Sur, Butarque and La Gavia, although this last one does not have any upstream actuator to be included in the improvement operation in the project.
- 6 flow input points:
  - In_D1 and in_D2: Inflow points from upstream the right margin interceptor. In this part the collector is doubled.
  - In_D3: Inflow from the tributary sewer getting into Oliva tank
  - In_D4: Inflow from the tributary sewer Butarque I
  - In_D5: Inflow from the tributary sewer Butarque II
  - In_I1: Inflow from upstream the left margin interceptor.
  - In_I2: Inflow from the tributary sewer getting into Abroñigales tank
- 5 CSO discharging points[1]:
  - CSO_D2: Right margin CSO point upstream main entrance to the Butarque tank
  - CSO_D3: CSO point located in the right margin interceptor upstream the Butarque WWTP.
  - CSO_D4: CSO point in Butarque II tributary sewer upstream the secondary entrance to the Butarque tank.
  - CSO_I1: CSO point in Abroñigales tanks
  - CSO_I2: CSO aliviadero sur point. In this point two discharging flows are met, the one coming from the effluent (and the non-treated waters bypassed in rainy events) from La Gavia WWTP, and the flow exceedance from the left margin interceptor.
- 6 flow output points to the WWTP:
  - WWTP_Butarque: Influent main line entrance to Butarque WWTP
  - WWTP_ButarqueP: Flows treated in the primary treatment line of the Butarque WWTP (it only operates in rainy events when the main line is working at full capacity).
  - WWTP_Gavia: Influent to Gavia WWTP.

[1] Considering WWTP Sur, an additional CSO point exists related to its by-pass at the entrance. Flows exceeding the hydraulic capacity of the plant are discharged to the environment.

- WWTP_Sur: Left margin interceptor drives the waters to the Sur WWTP. This WWTP treats these flows but also from other municipalities to the south of this point.

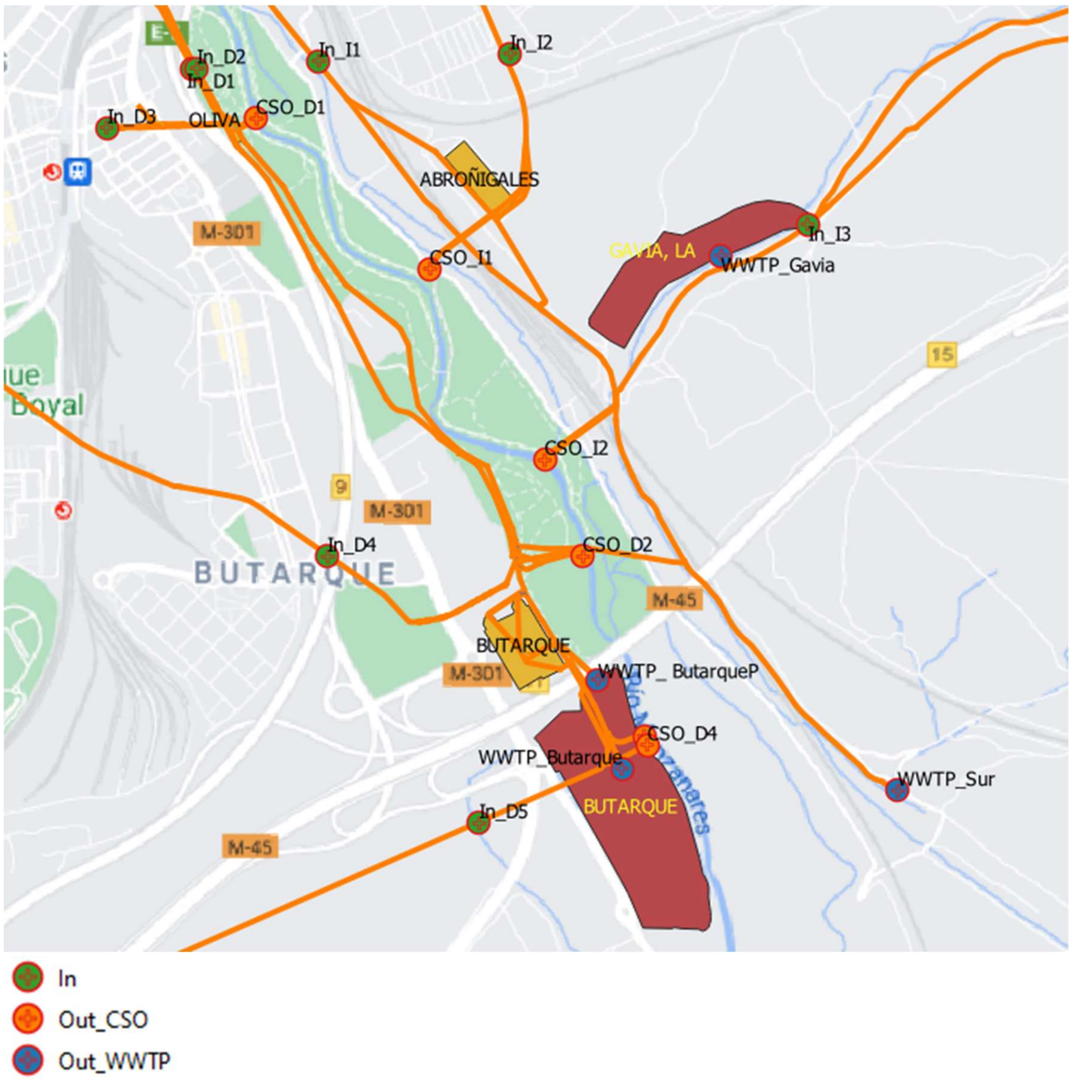

Figure 4 Location of the flow inputs and output points in the pilot site

In this pilot area, several operational management improvements have already been detected. The most important ones are related with the operation of the two main tanks in the area:

- Butarque tank: It has been checked that, during rain events, there are CSO discharges upstream of Butarque WWTP because its capacity is exceeded while the Butarque tank is far from being full.
- Abroñigales tank: Similarly, it has been verified that in rain events there are CSO discharges in Aliviadero Sur (located downstream the tank) while this tank is not full, and water is being by-passed.

As described in Chapter 2, the detailed model of the pilot network is very relevant for the software demonstrator in order to run the virtual tests (either using the MPC Controller or using the current operating rules used by the operator). Considering the pilot network characteristics mentioned above and their representation in GIS, in this project, the pilot network model has been adapted/developed from a previous version being transferred from Infoworks ICM to EPA SWMM (see deliverable DA1.2 for more details), which is the modelling tool used in this project. The model not only includes the network considered in the pilot area (Figure 4) but all the Manzanares system. In this sense, the network model outside of the pilot perimeter is operated using the current operating rules and it is used to forecast the inflows to the network inside the pilot perimeter (SWMM instance acting as a predictor of the pilot inflows), while the model inside the pilot perimeter is operated with either the computed MPC Controller strategy or the current operating rules (SWMM acting as a Virtual Reality) and is used to estimate the impacts on the environment of the control strategy.

In the following (Figure 5), the pilot network topology in EPA SWMM can be seen:

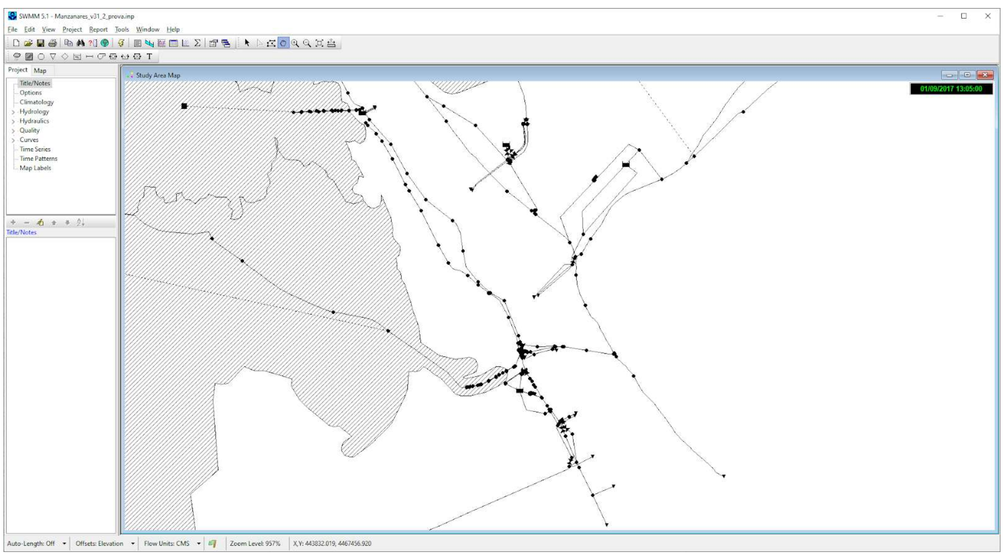

Figure 5 Network pilot topology on EPA SWMM

4.2 Description of the methodology to obtain the simplified model

As mentioned in Chapter 3, for the development of the MPC controller for RTC applications, it is very relevant to develop a simplified deterministic model of the pilot network with explicit equations to estimate accurately the spatial and temporal evolution of the main hydraulic and hydrology parameters (Puig et al., 2009). The detailed models representing hydraulic and hydrology complexities of urban drainage networks, and implemented in modelling tools as Infoworks ICM or EPA SWMM, are not feasible for RTC applications applying MPC.

For the purpose of RTC of urban drainage networks, a simple model structure should be used to represent the complex hydrology and hydraulics in sewer networks. The following principles (Puig et al., 2009) are followed:

- Representativeness of the main dynamics;
- Simplicity, flexibility, expendability and speed;
- Availability of on-line calibration and optimization.

As detailed in Chapter 3, the MPC methodology considered in the MPC Controller is based on solving an Optimal Control Problem (OCP) at every time instant *t*. In this context, simplified models are required to simulate large amounts of scenarios and control strategies and to evaluate the corresponding performance to choose the best one.

The computational efficiency of the optimizer may be degraded depending on the complexity and type of the equations included in the simplified formulation. Some mathematical expressions are not desirable for the optimizer because could make the optimizer unable to find a solution (optimum value), or even produce a wrong value. The following list contains the type of functions desirable for the optimizer (sorted by decreasing desirability).

- Linear functions
- Polynomial functions
- Logarithmic functions
- Exponential functions

The simplified model considered in LIFE RUBIES is a conceptual representation of the real hydrology / hydraulics associated with the pilot network, focusing mainly on those parts / variables which have a meaningful relevance on the overflows / effluents and associated contamination which are released to the receiving body (i.e. filling and emptying of the storage tanks, CSO points, inflows and effluents of the WWTPs). Mainly, the simplified model is developed considering mass-balance equations and certain data-driven expressions for specific hydraulics structures (i.e. weirs, gates with a constant position). All the parameters related to simplified model have been calibrated using a set of real rain events. The fact that at every time instant *t* (i.e. when solving the *OCP(t)* problem), the simplified model is fed with real measurements being used to provide variable estimations within a small time interval [t, t+6] (i.e. 30-minutal horizon prediction with a 5-minutal time step) guarantees the goodness of the computed forecasts. In addition, it is noticeable that the most relevant forecast is the one provided for *t+1* time instant.

In Figure 6, the relevant parts of the SWMM network pilot topology considered to generate the simplified model have been highlighted, while in Figure 7, the topology of the developed simplified model has been depicted.

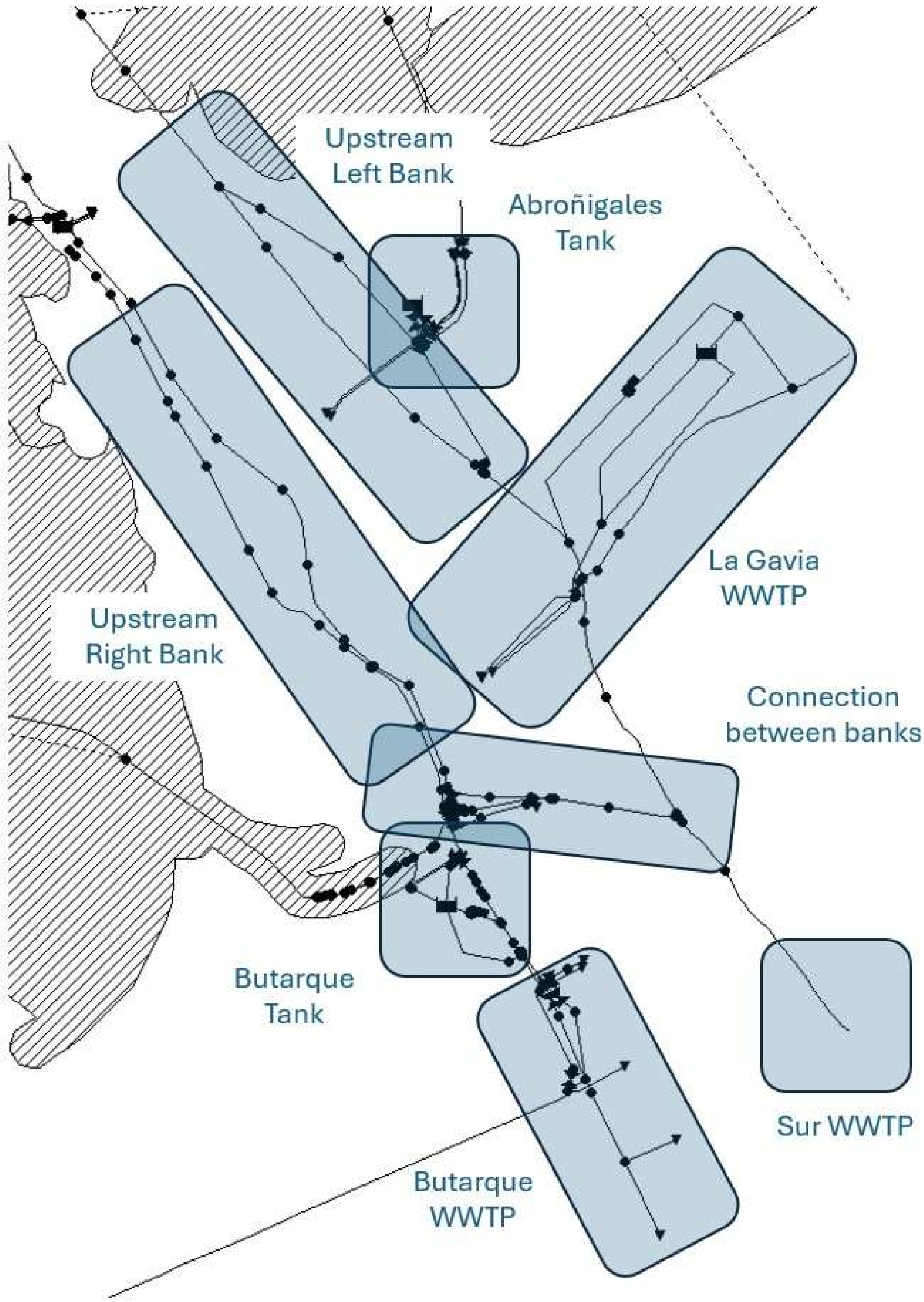

Figure 6 Network pilot topology on EPA SWMM: relevant parts considered to generate the simplified model

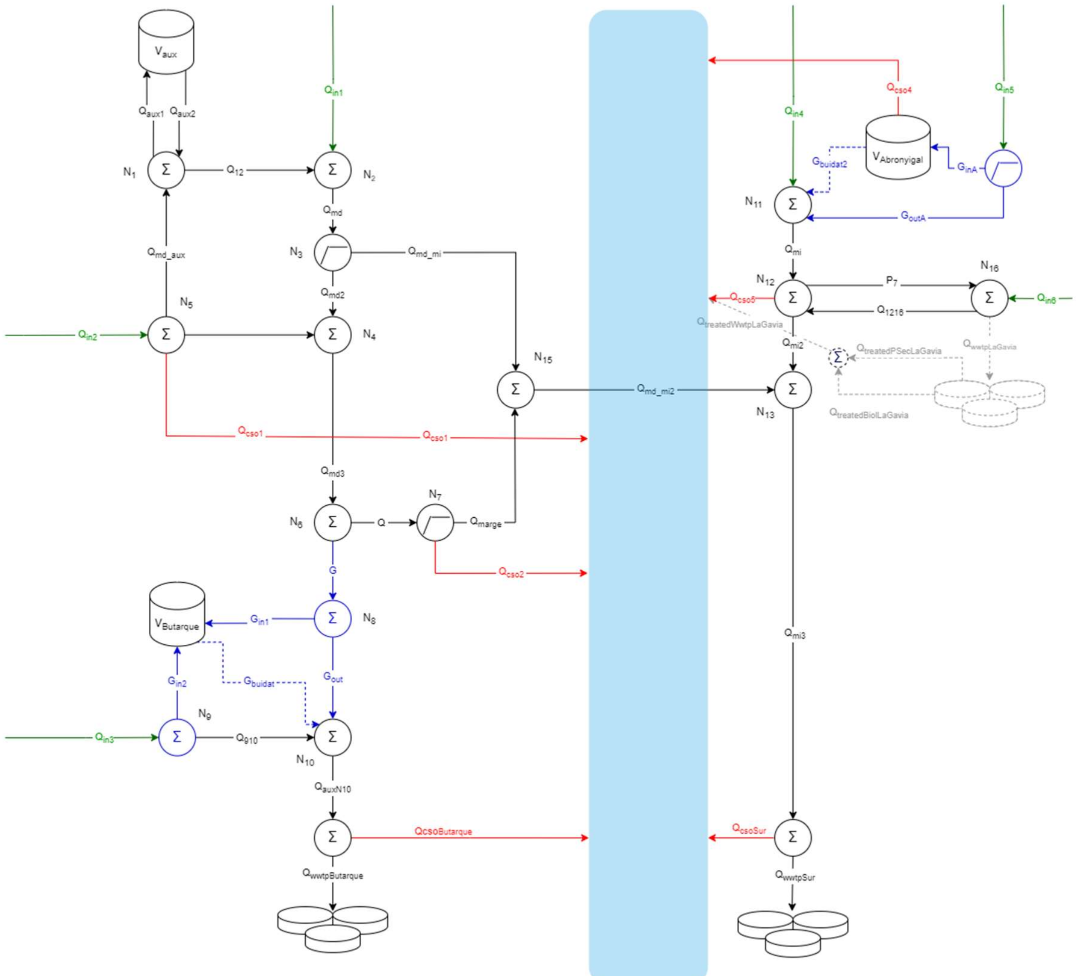

Figure 7 Network pilot topology of the resulting simplified model

In the following, sub-chapters, details of the development of the simplified model associated with pilot network will be given.

4.3 Simplified model – Details corresponding to the left bank of the Manzanares river

A complete representation of the simplified model for the left margin is provided at Figure 8. Let us describe the different components of this margin, emphasizing the differences between the detailed and simplified models.

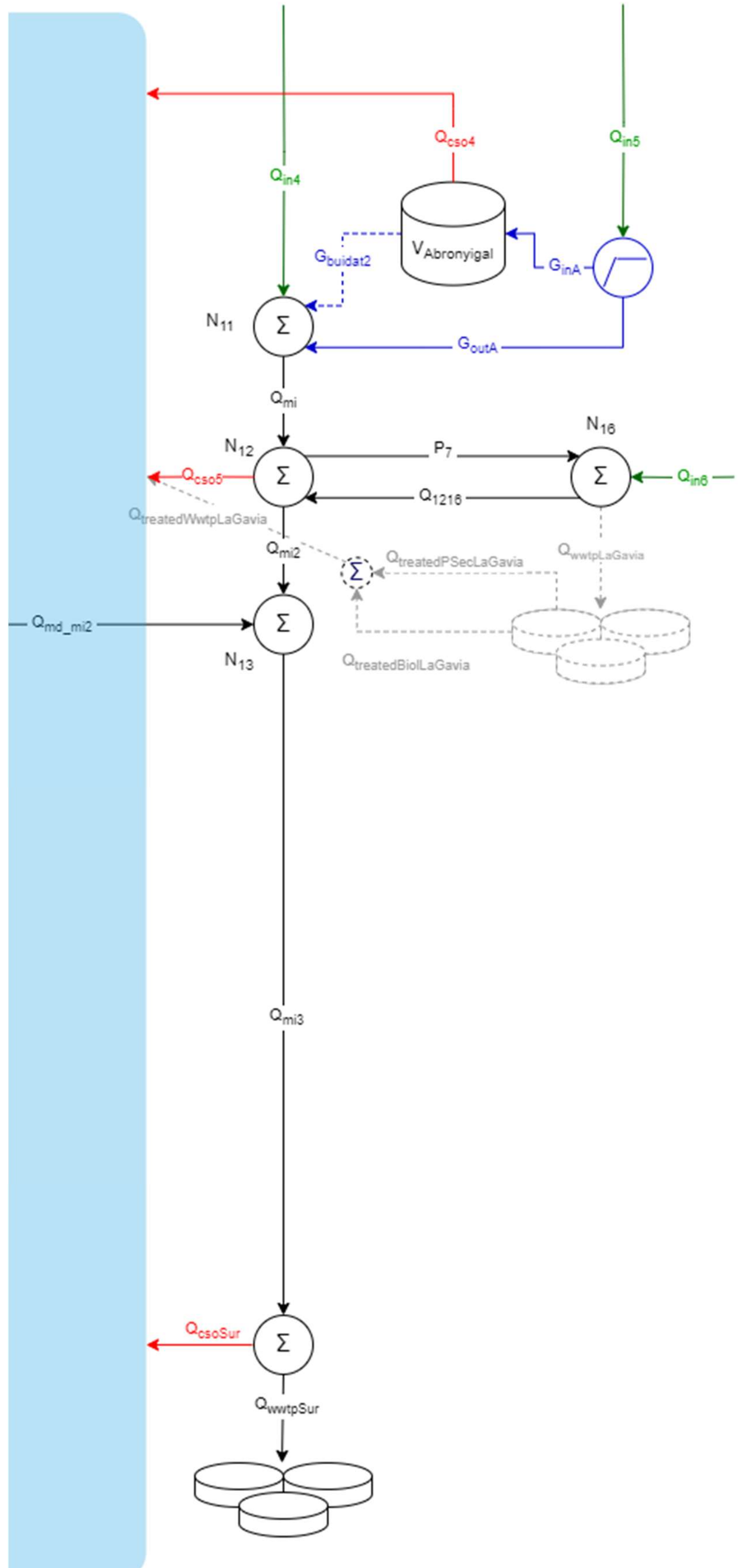
Q_cso4
Q_in5
Q_in4
V_Abronyigal
G_buidat2
G_inA
N_11
G_outA
Q_mi
N_16
N_12
P_7
Q_cso5
Q_in6
Q_1216
Q_treatedWwtpLaGavia
Q_mi2
Q_treatedPSecLaGavia
Q_wwtpLaGavia
Q_md_mi2
N_13
Q_treatedBiolLaGavia
Q_mi3
Q_csoSur
Q_wwtpSur

Figure 8 Complete representation of the simplified model for the left margin

4.3.1 Upstream Left Bank and Abroñigales Tank Model

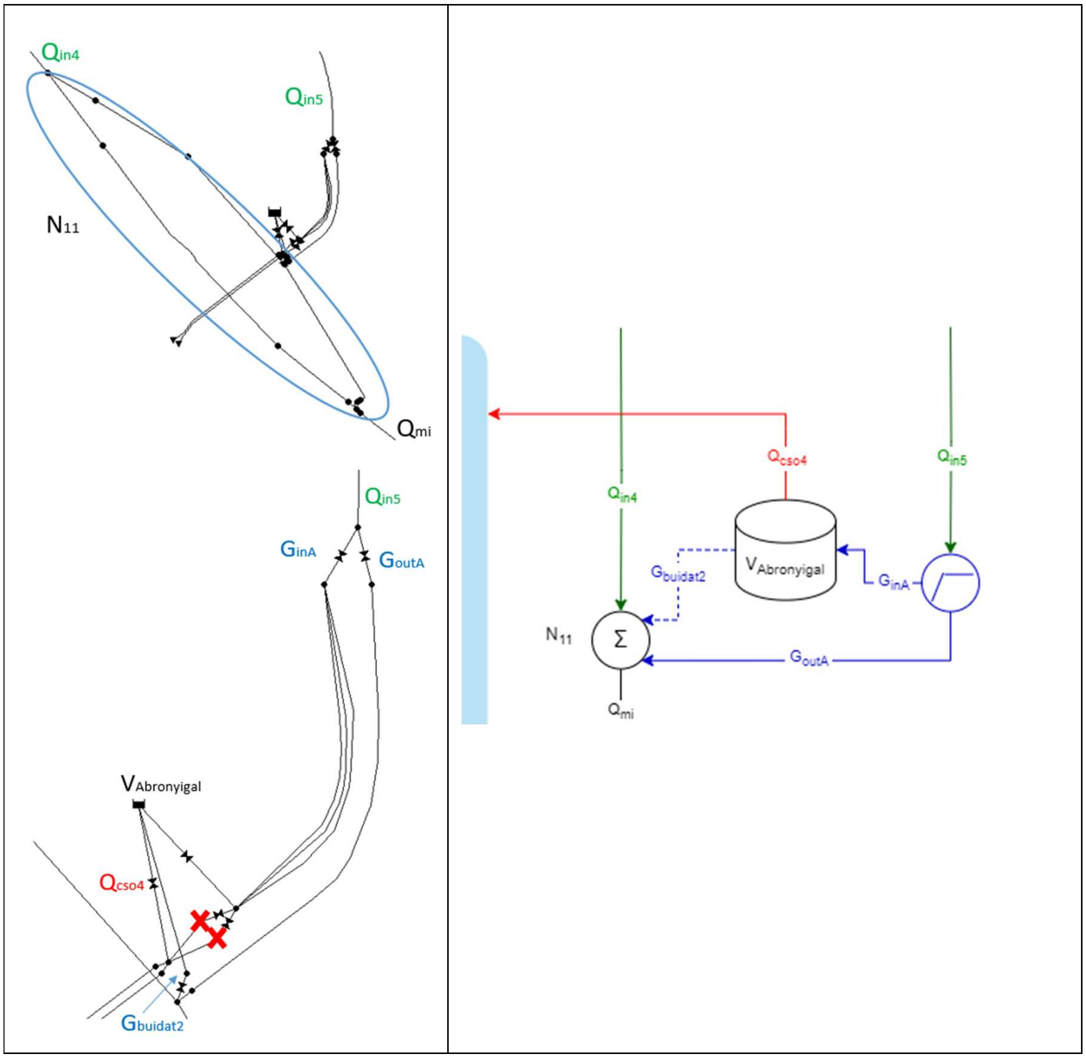

Figure 9 Detail of the SWMM model of the Upstream Left Bank and Abroñigales Tank and the corresponding diagram for the simplified model.

From the upstream left bank, the water entering through **Q_{in4}** is divided into two pipes in the detailed model: a first pipe conveys water to the area of the **$V_{Abronyigal}$** detention tank, whereas the second pipe bypasses the tank area. Note that this phenomenon is not represented in the simplified model, thus reducing the complexity of this representation (Figure 9). To this end, virtual node **N_{11}** is used to balance all the inflows and outflows of that part of the detailed network:

$$Q_{mi}(t) = Q_{in}(t) + G_{bu}(t) + G_{outA}(t)$$

The $\mathbf{V_{Abronyigal}}$ detention tank is the key control element in the left margin, as the rest of the elements are passive from a control perspective. The evolution of the volume inside the tank is described through an equation that relates the volume at the next time instant with the current volume and the inflows/outflows to the tank:

$$V_{Abronyigal}(t+1) = V_{Abronyigal}(t) + dt\big(G_{inA}(t) - Q_{CSO4}(t) - G_{buidat2}(t)\big)$$

There are two configurable actuators in this part of the network:

1. First, the water coming from $\mathbf{Q_{in5}}$ is divided into two different flows **(**$\mathbf{G_{inA}}$ and $\mathbf{G_{outA}}$**)** by means of a diversion gate, whose opening percentage can be settled as a setpoint. The former conveys water to the tank, whereas the latter bypasses it. Specifically, $\mathbf{G_{outA}}$ is used as the first actuator, thus selecting through as setpoint the proportion of $\mathbf{Q_{in5}}$ that is bypassed. The division of $\mathbf{Q_{in4}}$ into $\mathbf{G_{inA}}$ and $\mathbf{G_{outA}}$ is performed through the following equation:

$$G_{inA}(t) = Q_{in}\ (t) - G_{outA}(t)$$

2. The second actuator operates over the emptying of the tank through $\mathbf{G_{buidat2}}$. This corresponds to an orifice whose opening percentage can be configured as a setpoint. The tank emptying flow is limited in the simplified model through the current volume in the tank, so that the controller does not uses the tank as a pipe with delay:

$$0 \le G_{buidat2}(t) \le \frac{V_{Abronyigal}(t)}{dt}$$

The computed flows through these actuators must be converted into a setpoint (opening percentage) through a post-processing module, in order to feed the actuators in the next time instant. To this end, it is required to obtain an expression, for a set of opening setpoints, relating the flow through the input to the actuator and the outflow from this active element. Thus, when the optimization is solved and these flows for the next time instant are available, the distance from the point composed by the actual values and the different curves is computed, selecting the most similar one, and hence its associated setpoint.

The tank has an additional outflow through the CSO at $\mathbf{Q_{CSO4}}$**,** whose minimization is part of the goals pursued through the real-time control strategies. This CSO is computed as remaining flow that tries to enter the tank after a certain threshold level $\mathbf{V_{AbronyigalMax}}$ is reached:

$$Q_{CSO4}(t) = \frac{1}{dt}\max\Big(0,\ \Big(V_{Abronyigal}(t) + dt\big(G_{inA}(t) - G_{buidat2}(t)\big)\Big) - V_{AbronyigalMax}\Big)$$

Besides, note that there are two elements in the detailed model of the tank area that are not represented in the simplified version (marked with red crosses). This is justified because both elements are always closed in the real network.

4.3.2 La Gavia WWTP Model

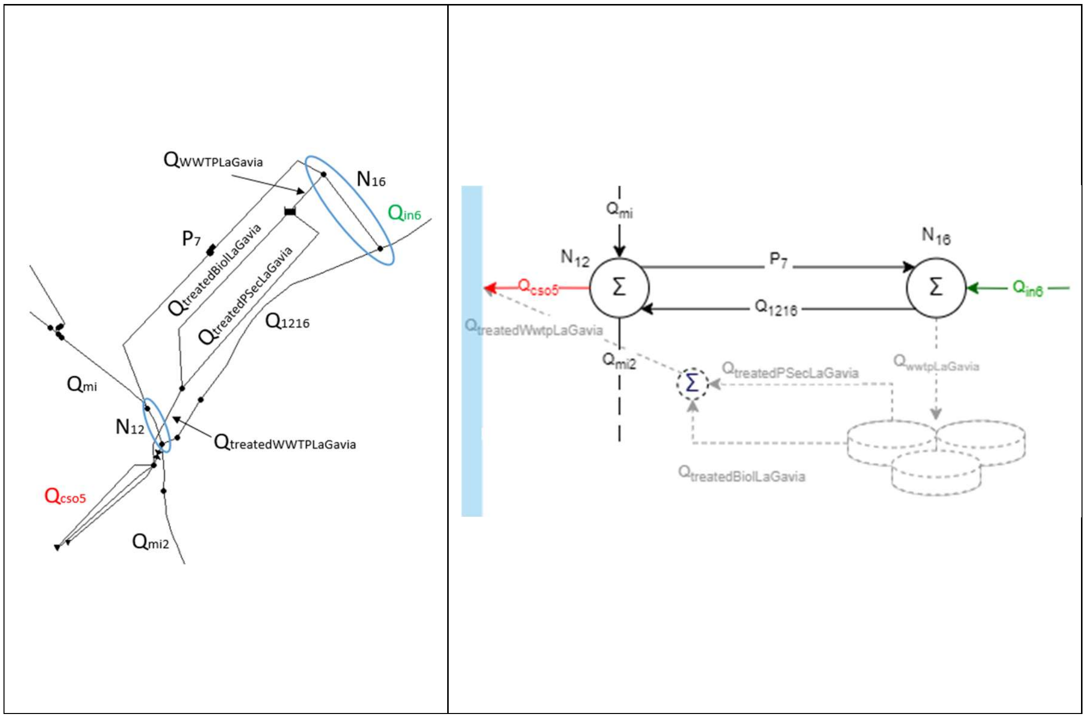

Figure 10 Detail of the SWMM model of the la Gavia WWTP and the corresponding diagram for the simplified model.

Another water inlet enters the margin through $\mathbf{Q_{in6}}$, whose flow is divided into water bypassed downstream **($\mathbf{Q_{1216}}$),** and water conveyed to the area of La Gavia WWTP (Figure 10). The relation between $\mathbf{Q_{in6}}$ and $\mathbf{Q_{1216}}$ is not direct, as there is not an active element that decides it. This relation was approximated through a data-based equation whose parameters are fitted using flow data from the available rain scenarios, and for all possible combinations of setpoints for the actuators $\mathbf{G_{outA}}$ and $\mathbf{G_{buidat2}}$ (considering a range from 0% to 100% of opening, with a step of 10%) (Figure 11):

$$Q_{1216}(t) = \max\left(0,\ 0.003Q_{in6}^{2}(t) + 0.921Q_{in6}(t) - 0.538\right)$$

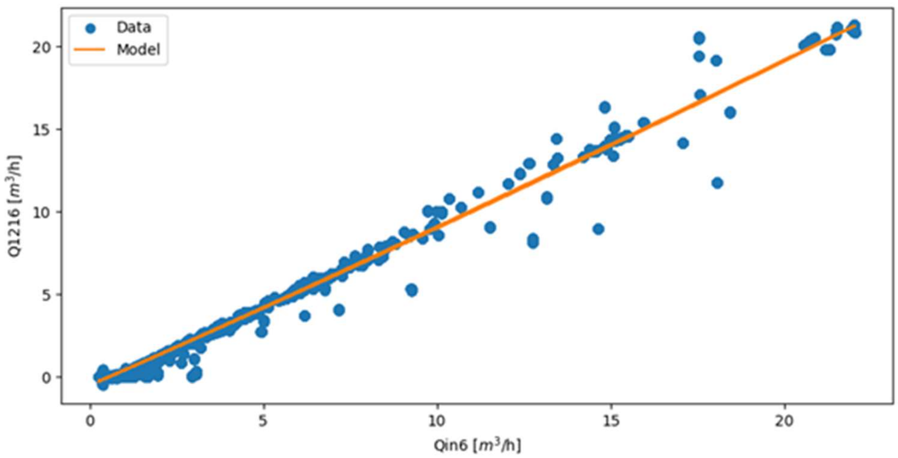

Figure 11 Fitting of the equation for flow Q1216 as a function of Qin6.

The balance at $\mathbf{N_{16}}$ allows to retrieve the water entering the WWTP, considering the flow coming from $\mathbf{Q_{in6}}$ that is not bypassed through $\mathbf{Q_{1216}}$, and the water pumped by means of the pump $\mathbf{P_7}$. Note that the inflow entering the WWTP is limited to 1.5 m^3/s:

$$Q_{WWTPLaGavia}(t) \ = \ \min\left(1.5, \ P_7(t) \ + \ (Q_{in} \quad - \ Q_{1216})\right)$$

Two outflows from La Gavia are represented in both the detailed and simplified models: $\mathbf{Q_{treatedBiolLaGavia}}$, which denotes the flow after leaving the facility after the biological treatment, and $\mathbf{Q_{treatedPSecLaGavia}}$, which stands for the flow leaving the WWTP after the secondary treatment. The former is limited to a maximum of 1.25 m^3/s, whereas the latter is the remaining flow when subtracted to the inflow to the WWTP:

$$Q_{treatedBiolLaGavia}(t) \ = \ \min\left(1.25, \ Q_{WWTPLaGavia}(t)\right)$$

$$Q_{treatedPSecLaGavia}(t) \ = \ Q_{WWTPLaGavia}(t) \ - \ Q_{treatedBiolLaGavia}(t)$$

Both are conveyed together, leading to the total outflow from the WWTP:

$$Q_{outWWPLaGavia}(t) \ = \ Q_{treatedPSecLaGavia}(t) \ + \ Q_{treatedBiolLaGavia}(t)$$

Regarding the balance of inflows and outflows at the virtual node $\mathbf{N_{12}}$ of the simplified model, a set of data-based equations is derived to obtain both the downstream flow $\mathbf{Q_{mi2}}$ and the part of $\mathbf{Q_{CSO5}}$ associated to $\mathbf{N_{12}}$ (which would be referred to as $\mathbf{Q_{CSO5.1}}$) through the values of the water coming from upstream ($\mathbf{Q_{mi}}$) and the bypassed flow from $\mathbf{Q_{in6}}$ to downstream **($\mathbf{Q_{1216}}$):**

$$Q_{mi2}(t) \ = \ -0.003Q_{1216}^2(t) \ - \ 0.041Q_{mi}^2(t) \ + \ 0.167Q_{1216}(t) \ + \ 0.874Q_{mi}(t)$$

$$Q_{CS \quad .1}(t) \ = \ 0.006Q_{1216}^2(t) \ + \ 0.042Q_{mi}^2(t) \ + \ 0.707Q_{1216}(t) \ + \ 0.155Q_{mi}(t)$$

The CSO flow $\mathbf{Q_{CSO5}}$ is then obtained through $\mathbf{Q_{CSO5.1}}$ and the outflow from La Gavia WWTP:

$$Q_{CSO5}(t) \ = \ Q_{CSO5.1}(t) \ + \ Q_{outWWTPLaGavia}(t)$$

Regarding the pump, in the detailed model it is an element whose behaviour is described by a pumping curve, which converts the water level of the node from which the pump extracts water to the pumped flow. This is a piecewise function, which cannot be explicitly represented in the optimizer. Thus, the pumping function is divided into two equations in the simplified model. First, a data-based equation uses the inflows/outflows to $\mathbf{N_{12}}$ to generate the level at the node where pump $\mathbf{P_7}$ is connected.

$$L_7(t) = -0.254Q_{mi2}(t) - 0.599Q_{CSO5}(t) + 0.583Q_{1216}(t) + 0.770Q_{mi}(t) + 0.868$$

Then, a second data-based equation tries to replicate the pumping curve, using in this case a sigmoid-based function (Figure 12).

$$P_7(t) = \frac{0.455}{0.883 + e^{-65.998L_7(t)+77.339}} + 0.132$$

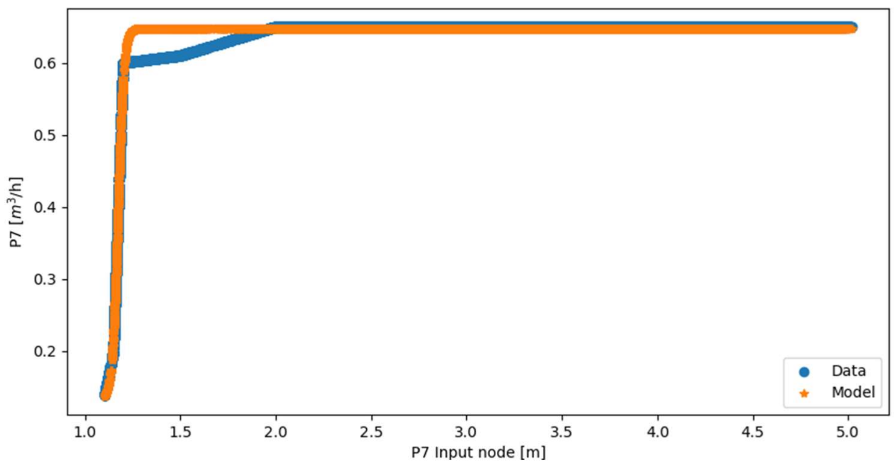

Figure 12 Fitting of the equation for flow P7 as a function of the inflow to node N12.

4.3.3 Connection between banks and Sur WWTP Model

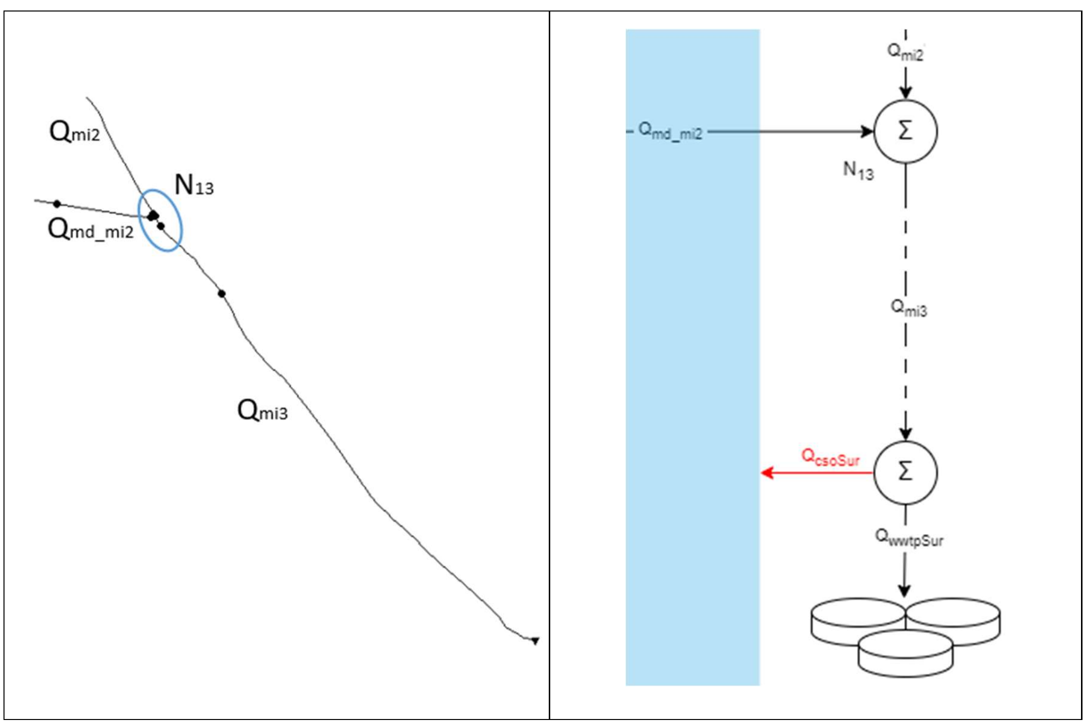

Figure 13 Detail of the SWMM model of the connection between banks and Sur WWTP and the corresponding diagram for the simplified model.

Finally, the water conveyed from the right margin through $\mathbf{Q_{md\_mi2}}$ is added to $\mathbf{Q_{mi2}}$, and this flow is conveyed to the Sur WWTP (Figure 13):

$$Q_{mi}\ (t) = Q_{mi2}(t) + Q_{mdmi}\ (t)$$

Despite it is not graphically represented in the scheme of the detailed model, the flow entering the Sur WWTP is limited to 6 m^3/s, and the rest of the incoming water is conveyed as CSO:

$$Q_{WWTPSur}(t) = \min\left(6, Q_{mi3}(t)\right)$$

$$Q_{CSOSur}(t) = Q_{mi3}(t) - Q_{WWTPSur}(t)$$

4.4 Simplified model – Details corresponding to the right bank of the Manzanares river

Figure 14 shows a diagram of the simplified model of the right-hand bank. Three inflows computed by the forecast module drive the model: Q_{in1} collecting the contribution of all urban upstream sub-catchments and Q_{in2} and Q_{in3} collecting the contribution from two individual sub-catchments at the southern part of the network.

The main control element in this part of the model is the Butarque Tank. Two sets of gates, G_{in1} and G_{in2}, can be used to fill the tank, one from the upstream part of the controlled area, G_{in1}, and one from the southern sub-catchment, G_{in2}. A third gate, G_{out}, can be used to control the water bypassing the tank. If both G_{in1} and G_{out} are closed, the water level along pipe G would increase until additional incoming flow is released through Q_{cso2} and Q_{marge}.

As usual with simplified models, most equations describe mass balances and only a few require fitting of nonlinear functions to describe the behaviour of hydraulic elements such as weirs. The modelling process has been divided in three stages: the upstream part of the controlled area, the Butarque tank and the downstream part of the controlled area, including the Butarque WWTP.

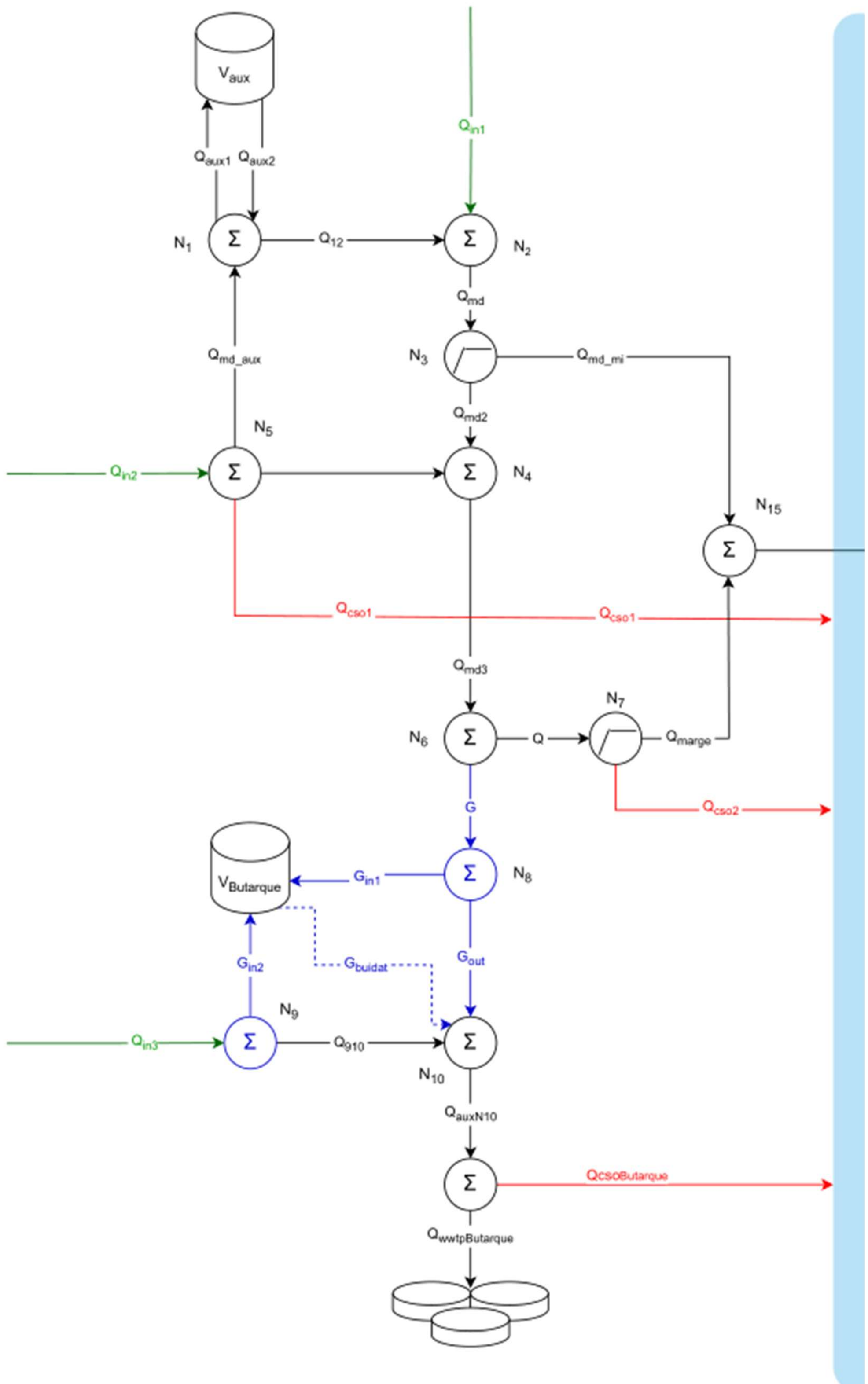
Vaux
Qaux1
Qaux2
N1
Q12
Qin1
N2
Qmd
N3
Qmd_mi
Qmd_aux
Qmd2
N5
Qin2
N4
N15
Qcso1
Qcso1
Qmd3
N7
N6
Q
Qmarge
G
Qcso2
VButarque
Gin1
N8
Gin2
Gbuidat
Gout
N9
Qin3
Q910
N10
QauxN10
QcsoButarque
QwwtpButarque

Figure 14 Simplified model of the right-hand bank of the controlled area.

4.4.1 Upstream Right Bank Model

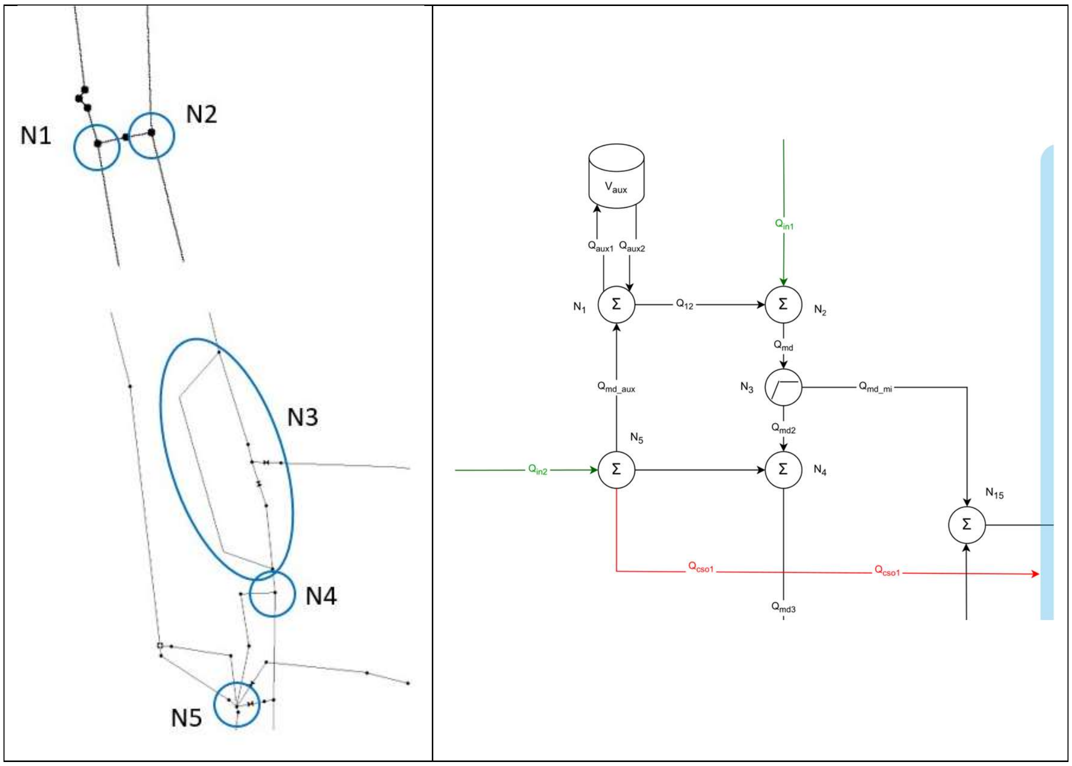

Figure 15 Detail of the SWMM model of the upstream right bank and the corresponding diagram for the simplified model.

The upstream part of the right bank does not contain any control elements (Figure 15). The most important inflow is Q_{in1}, which comes from the upper part of the network. At node N_1 Q_{in1} joins part of the second inflow Q_{in2} which flows to the north through pipe Q_{md_aux}. In node N_3 part of this total inflow is diverted to the left-hand bank. The equation for node N3 has been fitted to data from several rain events as follows (Figure 16):

$$Q_{md\_mi} = \min\{\, 0.166 \cdot Q_{md} - 0.144,\ 0.023 \cdot Q_{md} + 0.533 \,\}$$

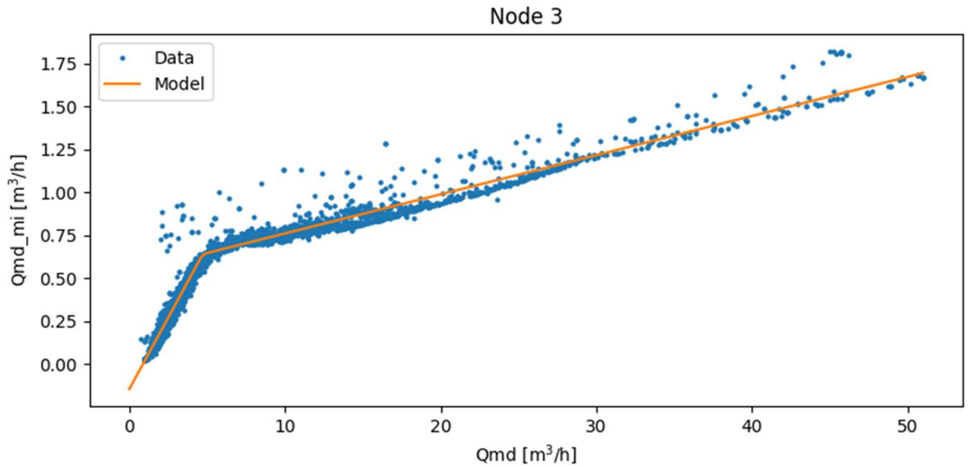

Figure 16 Fitting of the equation for flow Qmd_mi as a function of Qmd.

Similarly, node N5 has the following fitted equations (Figure 17; Figure 18):

$$Q_{45} = 1.529 \cdot \max\{ 0, Q_{B1} - 2.143 \}^{0.653}$$

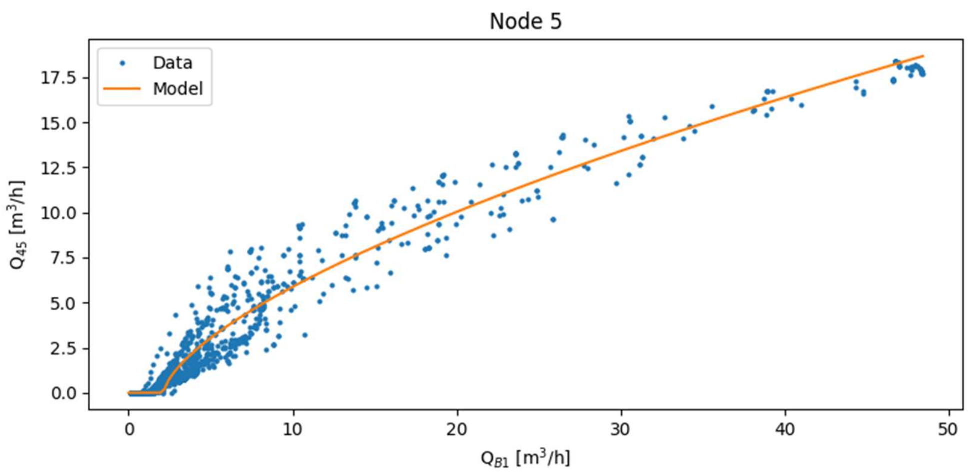

Figure 17 Fitting of the equation for flow Q45 as a function of QB1.

$$Q_{cso1} = \max\{ 0, 0.226 \cdot Q_{B1} - 6.606 \}$$

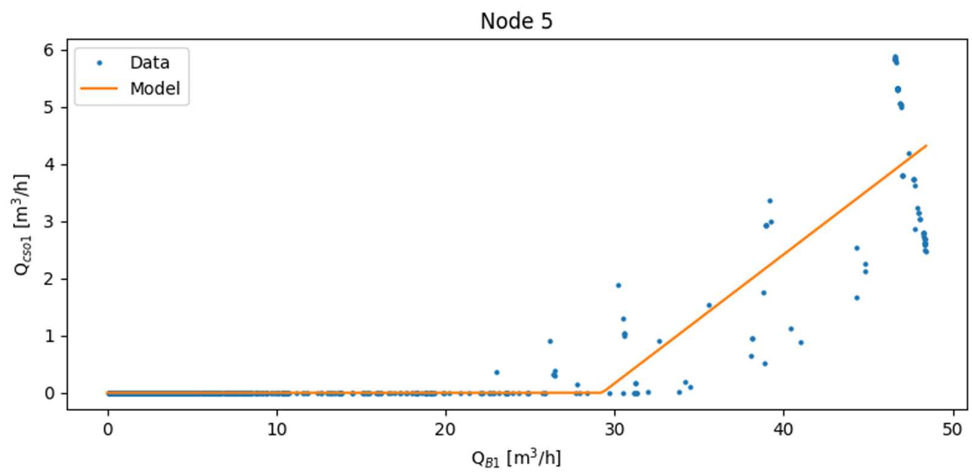

Figure 18 Fitting of the equation for flow Qcso1 as a function of QB1.

Finally, virtual tank V_{aux} is used to mimic the behaviour of water flowing upstream through pipe Q_{md_aux} during the peak flow instants and later flowing downstream again through pipe Q_{12}.

4.4.2 Butarque Tank and WWTP Model

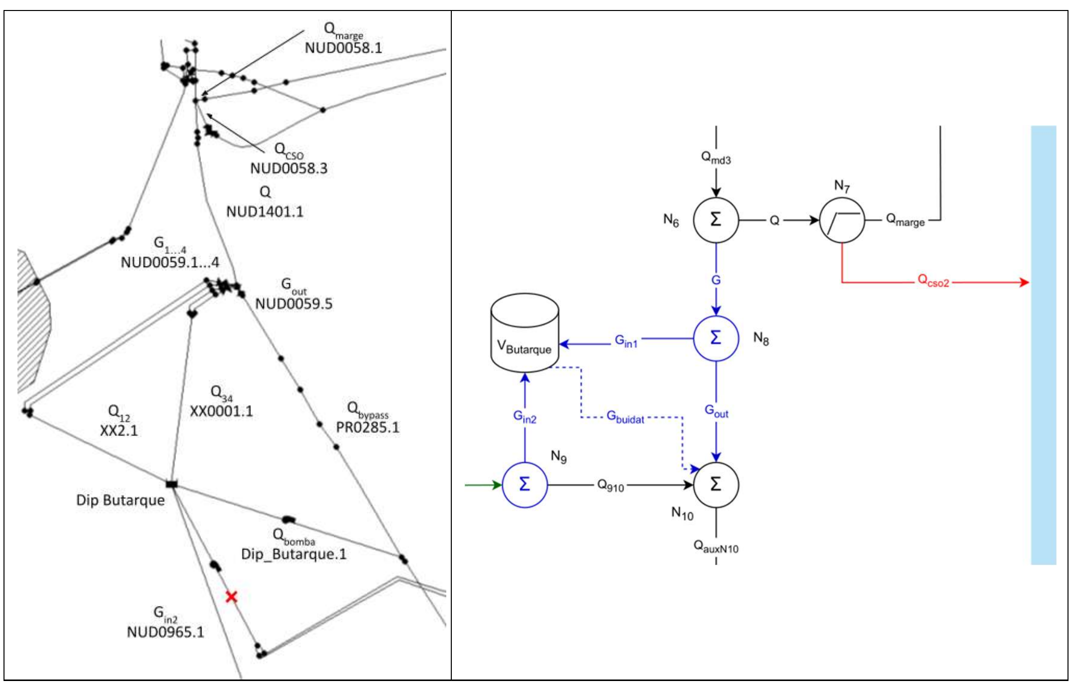

Figure 19 Detail of the SWMM model of the Butarque Tank and WWTP and the corresponding diagram for the simplified model.

This is the part of the right-hand bank that contains the Butarque tank, together with the gates that are used to either fill or bypass it (Figure 19). A little upstream of the tank, a weir structure can divert part of the water reaching the tank to the left-hand margin (Q_{marge}) and, if the level is high enough to a CSO (Q_{cso2}). These two flows are modelled using minimum and maximum functions as follows (Figure 20; Figure 21):

$$Q_{marge} = \min\{ Q, 0.05 \cdot Q + 4.07 \}$$

$$Q_{cso2} = \max\{ 0, 0.95 \cdot Q - 4.07 \}$$

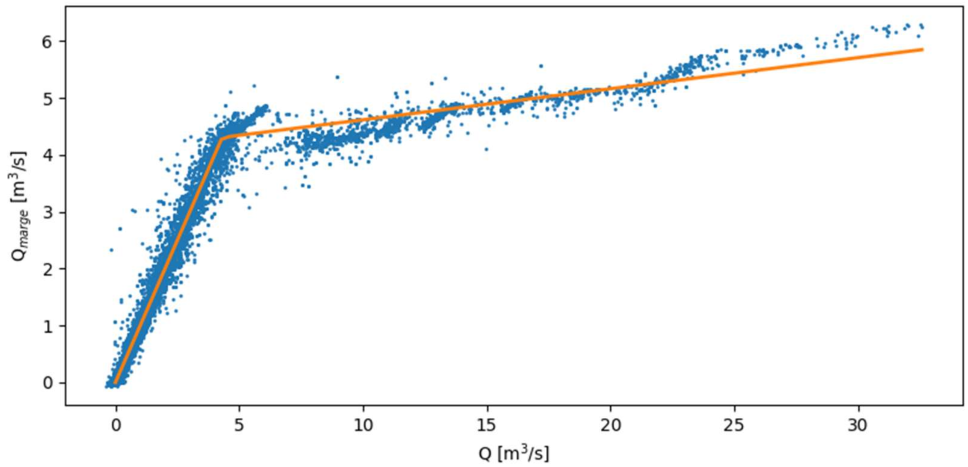

Figure 20 Fitting of the equation for flow Q_{marge} as a function of Q.

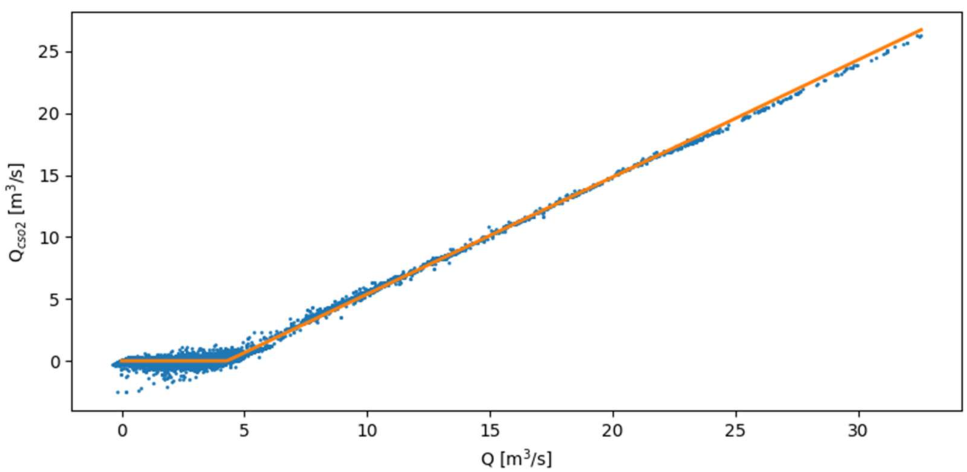

Figure 21 Fitting of the equation for flow Q_{cso2} as a function of Q.

4.4.3 Downstream Right Bank and Butarque WWTP Model

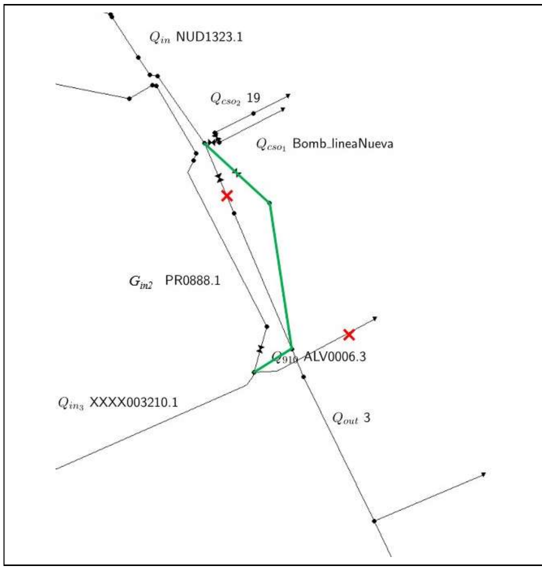

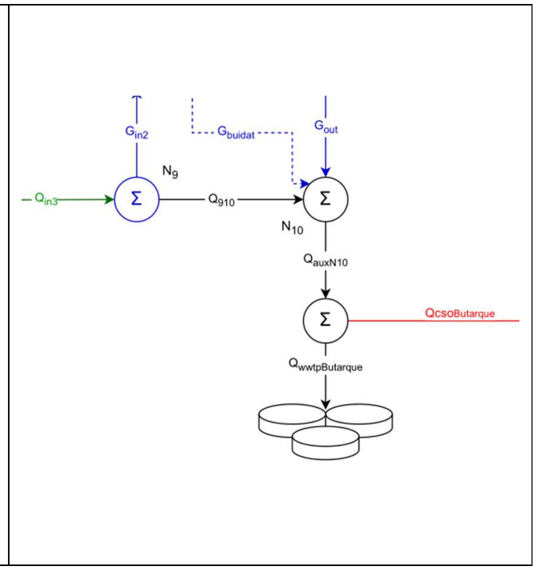

Figure 22 Detail of the SWMM model of the right bank and Butarque WWTP and the corresponding diagram for the simplified model.

The Butarque WWTP can be found at the downstream end of the right bank collector (Figure 22). It receives the flow form the right bank collector (G_{out}) and from a catchment at the south-west part of the network (Q_{in3}). There are two links in this part of the network that never carry any water, marked with a red cross on the diagram: the first one is a gate which is always closed during wet weather, the second one is a 1.75m high weir that never activates for the tested rains.

The south catchment Q_{in3} is divided into a part controlled by a gate and routed towards the Butarque tank G_{in2}; and another towards the Butarque WWTP Q_{910}:

$$Qin3 = Gin2 + Q910$$

For the simplified model, the three links shown in green in Figure 22 are collapsed into a single node N10 collecting the upstream right bank (G_{out}), the south catchment (Q_{910}) and the tank emptying (G_{buidat}, not considered in the current simulations) contributions:

$$Q_{auxN10} = Q_{910} + Gout + G_{buidat}$$

This total inflow is used to compute the CSO occurring at the WWTP inlet $Q_{csoButarque}$ and the treated flow $Q_{wwtpButarque}$. The equation for the CSO structure was fitted to simulation data as follows (Figure 23):

$$Q_{csoButarque}(t) = \max \{ 0, 0.88 \cdot Q_{auxN10}(t\text{-}3) - 3.44 \}$$

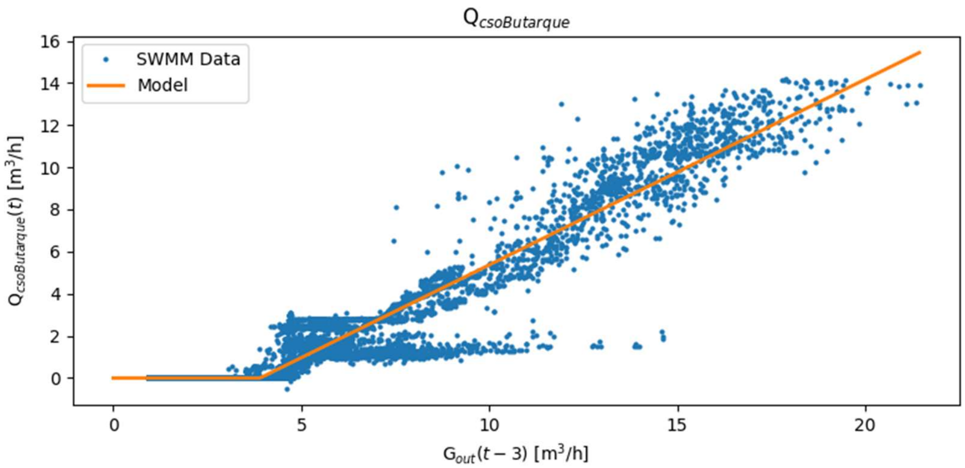

Figure 23 Fitting of the equation for flow QcsoButarque as a function of Gout.

Finally, the treated flow can be computed as follows, using the WWTP maximum capacity of 4 m^3/s:

$$Q_{wwtpButarque} = \min \{ Q_{auxN10}(t), 4 \}$$

5 Test results – MPC controller performance

5.1 Introduction

In this chapter, the performance of the MPC Controller (Chapter 3) has been compared with the Local Control Rules, integrated in the hydraulic model provided by the operator using the software demonstrator (Chapter 2), and considering a set of 9 real rains. Mainly, this comparison is based on the CSO volumes released to the environment, storage volume in the tanks at the end of the rain event and volumes of water treated at the WWTP during the whole scenario. The software demonstrator allows to compute the indicators for every considered rain event. Then, these indicators are aggregated considering all rain events to provide global indicators for the MPC Controller and for the Local Control Rules.

In sub-chapter 5.2, the main characteristics of the considered rain events are provided; while in sub-chapter 5.3, the global indicators comparing the two controllers for all the used rain events are given. Finally, for a specific rain event, the hydraulic dynamics of the relevant variables in the pilot network corresponding to the MPC Controller and the Local Control Controller can be seen.

5.2 Rain events scenarios

To test the MPC controller and compare its performance against the current operation rules, rain gauge data corresponding to years 2016 and 2017 has been analysed to select the highest intensity events. Figure 24 shows the intensity time-series with the selected events highlighted in different colours.

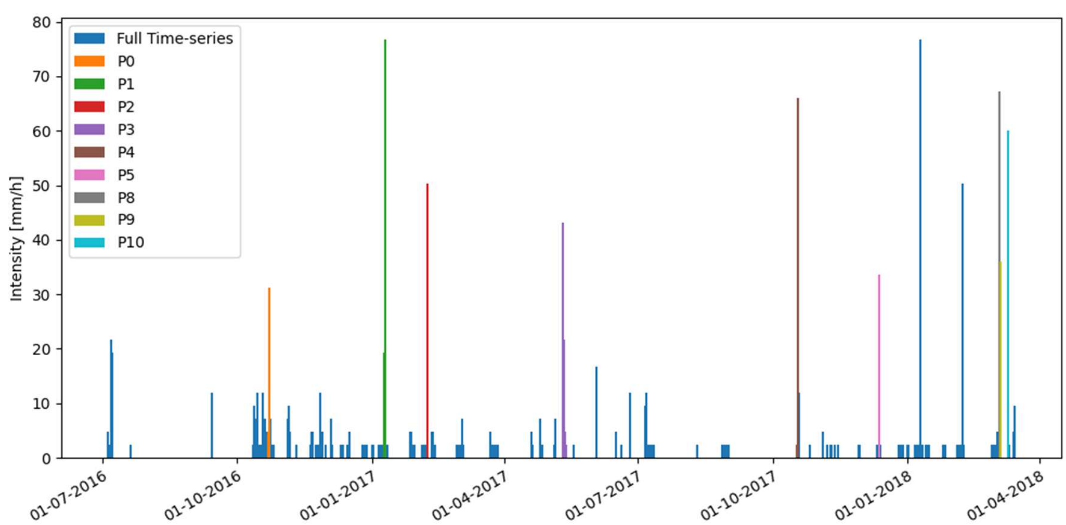

Figure 24 2016 and 2017 rain time series with highlighted rain events used for controller evaluation.

Table 1 shows the main properties of the selected rain events and Figure 25 shows more detailed plots of the selected events:

Rain Event	P [mm]	Imax [mm/h]	Date	Duration
P0	17.0	31.2	2016-10-22	10h 10min
P1	35.8	76.8	2017-01-09	17h 20min
P2	23.6	50.4	2017-02-07	05h 35 min
P3	21.6	43.2	2017-05-10	1 day 22h 55 min
P4	24.1	66.0	2017-10-17	15h 35 min
P5	15.4	33.6	2017-12-12	3h 50 min
P8	15.8	67.2	2018-03-04	1h 45 min
P9	21.3	36.0	2018-03-04	13h 45 min
P10	19.4	60.0	2018-03-10	01h 5 min

Table 1 Precipitation, maximum intensity, date and duration of the selected rain events.

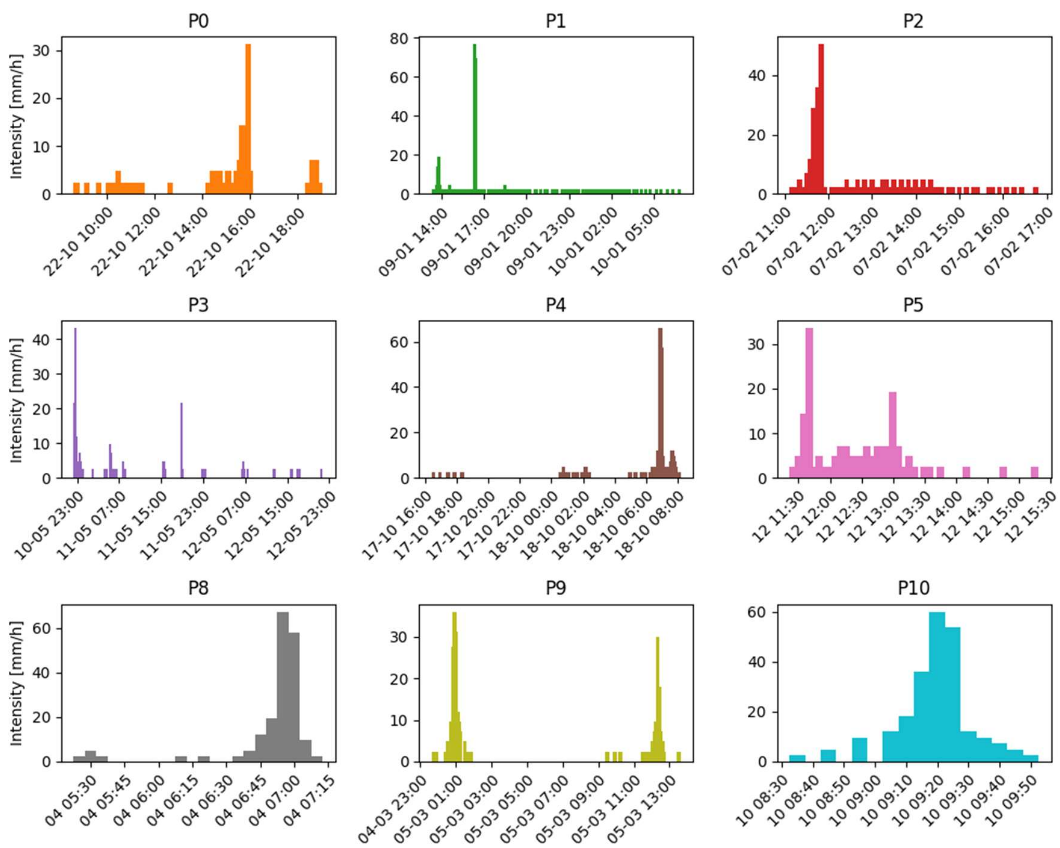

Figure 25 Intensity of the selected rain events.

5.3 Overall results / performance

Three main Key Performance Indicators (KPI) have been considered to evaluate and compare the two proposed control strategies:

- Combined Sewer Overflow Volume [$10^3 \cdot m^3$]: the total water volume released from the drainage network to the Manzanares river through the different structures designed to do so.
- Treated WWTP Volume [$10^3 \cdot m^3$]: the total water volume reaching WWTPs. At this point it is considered that all volume reaching a WWTP is fully treated and can be released to the environment with no pollution effect.
- Tank volume at the end of the event [$10^3 \cdot m^3$]: as mentioned earlier, this set of simulations does not account for emptying of storm tanks. The volume stored in storm tanks at the end of the event is to be considered as water that will eventually be routed to a WWTP during wet weather and thus will cause no pollution effect on the environment.

These volumes are computed using the results of the SWMM model. Table 2 lists the SWMM model elements that have been used to compute the KPIs:

KPI	SWMM Element	Notes
CSO_1	NUD1377.1	Link
CSO_2	PR0291.2	Link
CSO_3	Comp_lineanueva	Link
CSO_4	Abronyigal.1	Link
CSO_5	NUD0943.1	Link
CSO_6	NUD0939.1	Link max{ 0, flow(NUD0939.1) - 6 }, only the flow exceeding the Sur WWTP capacity of 6 m^3/s is considered CSO.
Butarque WWTP	3	Link
Sur WWTP	NUD0939.1	Link min{ 6, flow(NUD0939.1) } only the flow below the Sur WWTP capacity of 6 m^3/s is considered treated.
Butarque Tank	Dip_Butarque	Tank
Abroñigales Tank	Abronyigal	Tank

Table 2 SWMM variables used for the computation of KPIs.

After running the MPC closed-loop simulation algorithm and the rule-based control simulations for each rain event, the different KPI volumes have been computed and compared. Table 3 shows the relative variation of volumes between the MPC controller and the rule-based controller, using the rule-based controller as baseline:

$$\text{Relative Variation} = (KPI_{MPC} - KPI_{Rules}) / KPI_{Rules} \cdot 100\ [\%]$$

Rain Event	Relative CSO Variation	Relative WWTP Variation	Relative Tanks Variation
P0	-36 %	1 %	99 %
P1	-7 %	0 %	11 %
P2	-23 %	3 %	34 %
P3	-35 %	-2 %	115 %
P4	-36 %	0 %	70 %
P5	-39 %	1 %	80 %
P8	-51 %	4 %	75 %
P9	-40 %	-2 %	80 %
P10	-46 %	3 %	73 %

Table 3 Relative difference of the KPIs obtained by the MPC controller and the current operation rule-based controller for the different rain events.

Similarly, Figure 26 shows the different KPI volumes for each simulated rain event in $10^3 \cdot m^3$:

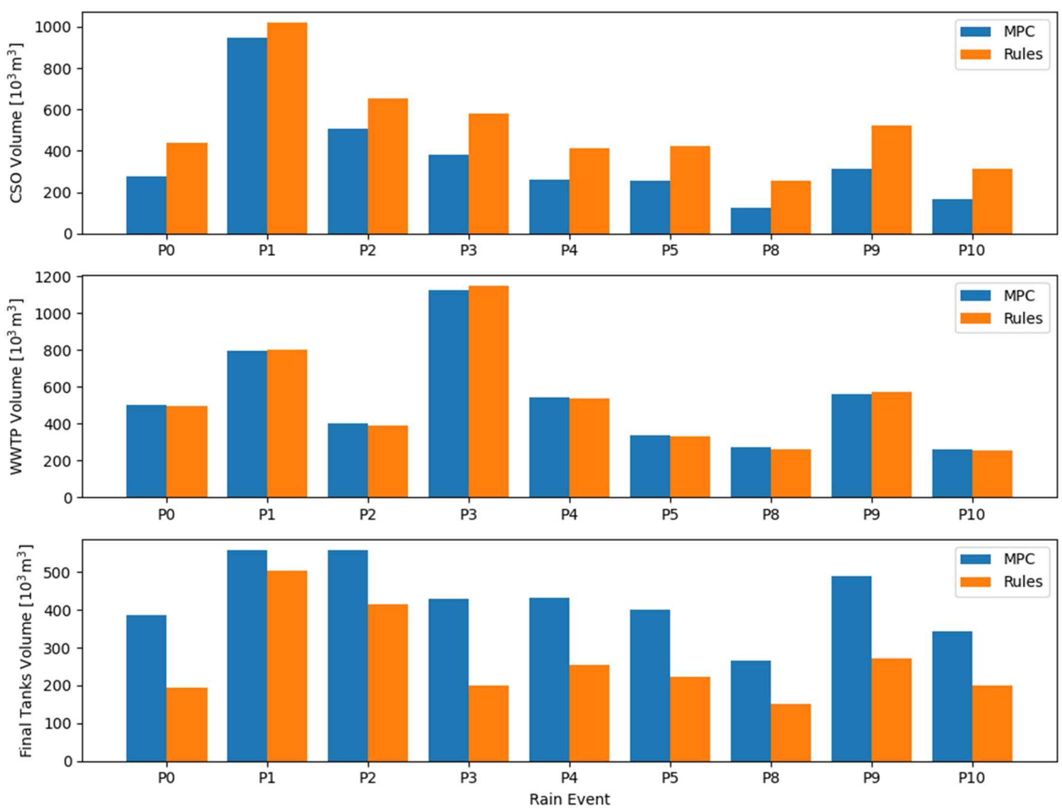

Figure 26 KPI volumes obtained by the MPC controller and the current operation rule-based controller for the different rain events.

The MPC controller can reduce CSO volumes in all scenarios by routing larger volumes to the storm tanks. Treated wastewater volumes are almost identical for both controllers since WWTPs work at maximum capacity during rain events. Wastewater volume at the end of the events is to be considered as potentially treated water during a following wet weather period and would eventually be added to the WWTPs treated volume.

Detailed results for each rain event and each KPI can be found in Table 9, Table 10 and Table 11 in Appendix 7.1.

5.4 Details of the results for a given rain scenario

In this section the results for rain event P0 will be described in more detail. Rain event P0 is moderate event lasting for about 12 hours and reaching a peak intensity of 31 mm/h (Figure 27).

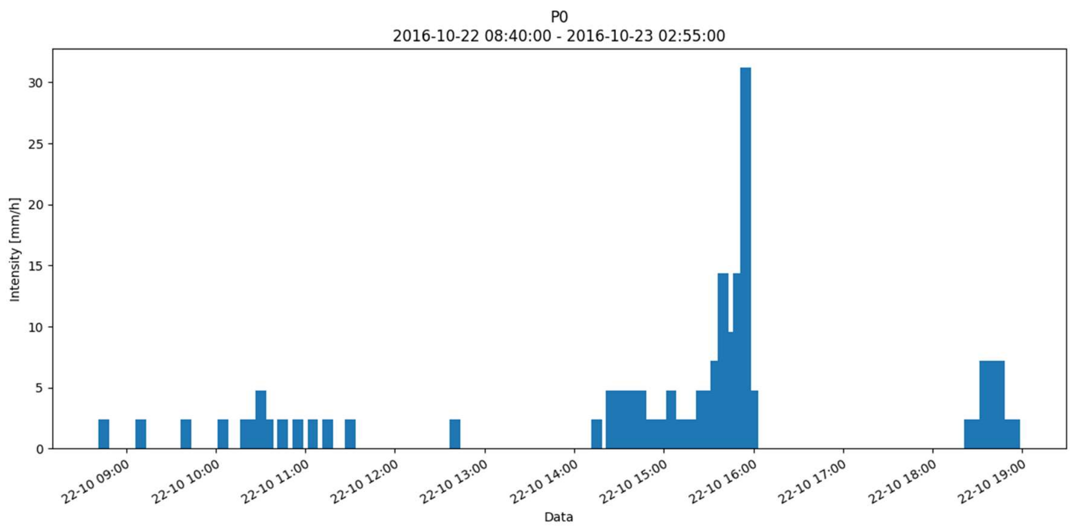

Figure 27 Rain event P0 rain intensity.

The runoff caused by the rainfall over the whole model area results into the six inflows entering the controlled area shown in Figure 28. There is a slight mismatch between MPC and rules simulation inflow Q_{in4} due to some accumulation in the pipe caused by the rule-based controller. This difference, however, is not expected to have a relevant impact in any of the presented results.

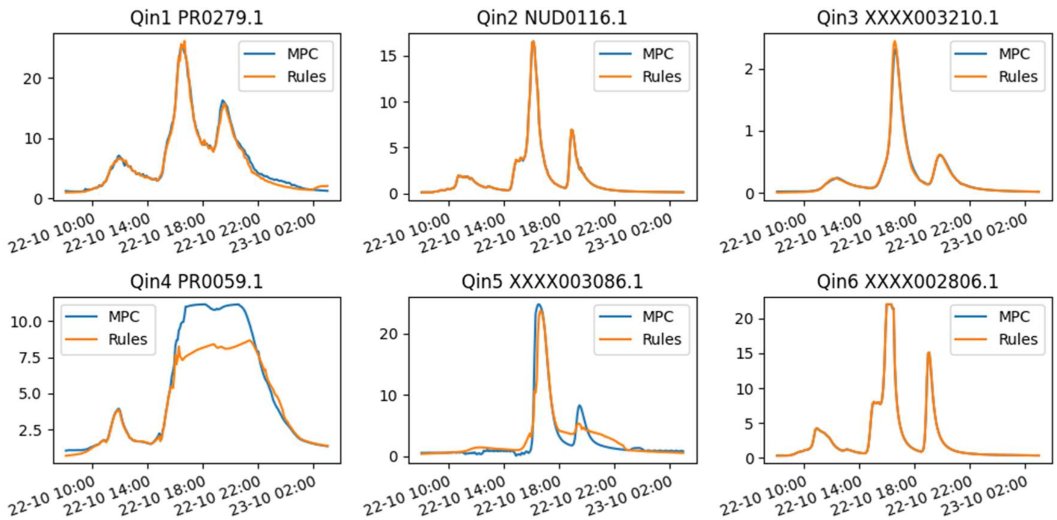

Figure 28 Controlled area inflows during rain event P0 obtained by the MPC controller and the current operation rule-based controller for the different rain events.

Table 4 shows the mass balance in the controlled area. Considering that all incoming volume during the simulation period must end either in a CSO structure, a WWTP or a Tank, the difference between total inflow and total outflow corresponds to water volume kept inside the controlled area pipes.

	Mass Balance MPC [$10^3 m^3$]	Mass Balance Rules [$10^3 m^3$]
Total Inflow	1275	1221
Total Outflow (CSO + WWTP + Tanks)	1166	1129
Difference	109	92

Table 4 Mass balance of the controlled area network during the simulation of rain event P0 as obtained by the MPC controller and the current operation rule-based controller for the different rain events.

Table 5 shows the main KPIs associated with the simulation of rain event P0 for both the MPC and the Rule-based controllers. The MPC controller can reduce CSO spills by $160 \cdot 10^3$ m^3 with respect to the rule-based controller. This reduction is mainly due to the additional $192 \cdot 10^3$ m^3 that are stored in detention tanks.

	MPC Volume [$10^3 m^3$]	Rules Volume [$10^3 m^3$]	Absolute Volume Variation [$10^3 m^3$]	Relative Volume Variation [%]
CSO	278	438	-160	-36
WWTP	503	498	5	1
Tanks	386	193	192	99

Table 5 KPI volumes for rain event P0 obtained by the MPC controller and the current operation rule-based controller for the different rain events.

5.4.1 Combined Sewer Overflows

There are two CSO points in which the MPC controller can reduce the CSO flow to the Manzanares river with respect to the current operation, as shown in Table 6. Both correspond to the CSO structures immediately downstream of the two detention tanks. The MPC controller is more flexible in adapting the gate positions to route larger volumes to the detention tanks thus reducing the downstream flowrate, preventing higher water levels and activation of CSO weirs.

	MPC Volume [$10^3 m^3$]	Rules Volume [$10^3 m^3$]	Difference [$10^3 m^3$]
CSO_1	0	0	0
CSO_2	0	0	0
CSO_3	0	104	-104
CSO_4	0	0	0
CSO_5	239	292	-53
CSO_6	39	42	-3
Total	278	438	-160

Table 6 Total CSO volumes for rain event P0 obtained by the MPC controller and the current operation rule-based controller for the different rain events.

Figure 29 shows the CSO flowrate time-series for each CSO point, where it can be noticed that CSO_3 flow, downstream of Butarque tank, can be completely avoided. CSO_5, downstream of Abroñigales tank can only be slightly reduced, since part of the flow reaching the tank is always bypassed even if the inflow gate is completely open.

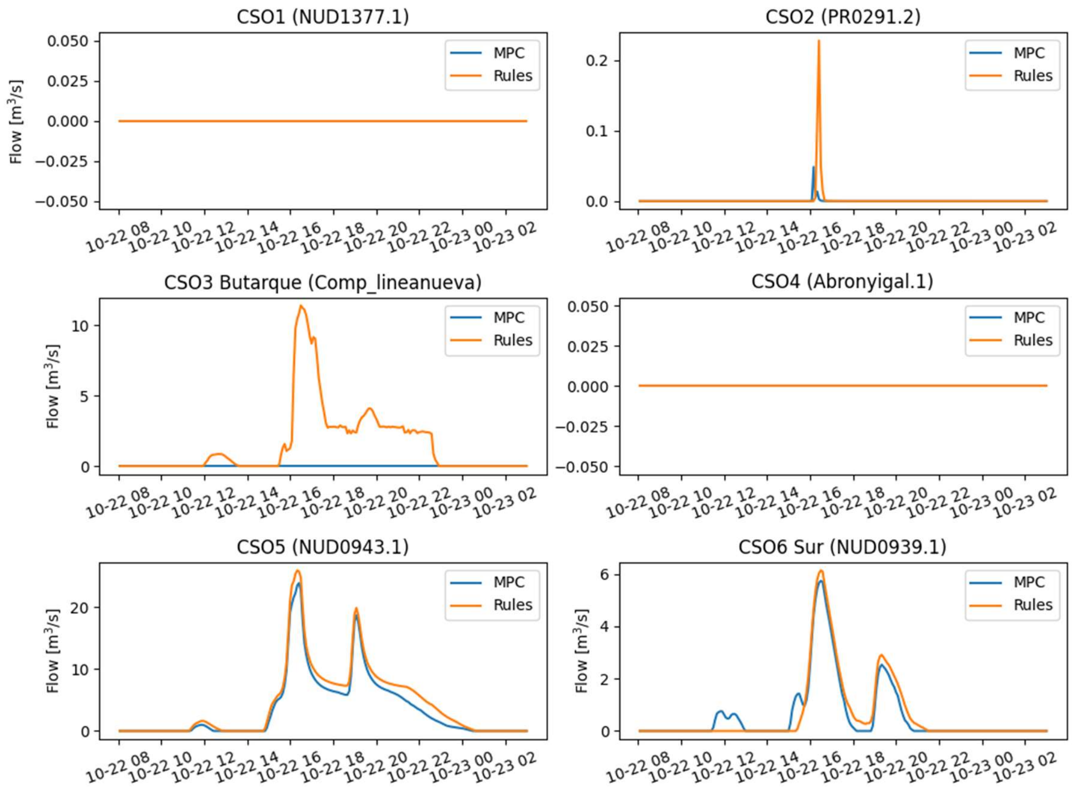

Figure 29 CSO flows during rain event P0 obtained by the MPC controller and the current operation rule-based controller for the different rain events.

5.4.2 Tank Usage

As mentioned in the previous section CSO reduction by the MPC controller is mainly attained by routing larger wastewater volumes to the detention tanks. Table 7 and Figure 30 illustrate this phenomenon. The stored wastewater in the two detention tanks at the end of the event is almost 10^5 m^3 larger for the MPC controller. This stored volume can be slowly released towards the corresponding WWTPs once the rain event is over, and the network flowrates return to the dry weather ones.

	MPC Volume [$10^3 m^3$]	Rules Volume [$10^3 m^3$]	Difference [$10^3 m^3$]
Butarque Tank	242	148	94
Abroñigales Tank	143	46	97
Total	386	193	192

Table 7 Volume stored in detention tanks at the end of the simulation of rain event P0 obtained by the MPC controller and the current operation rule-based controller for the different rain events.

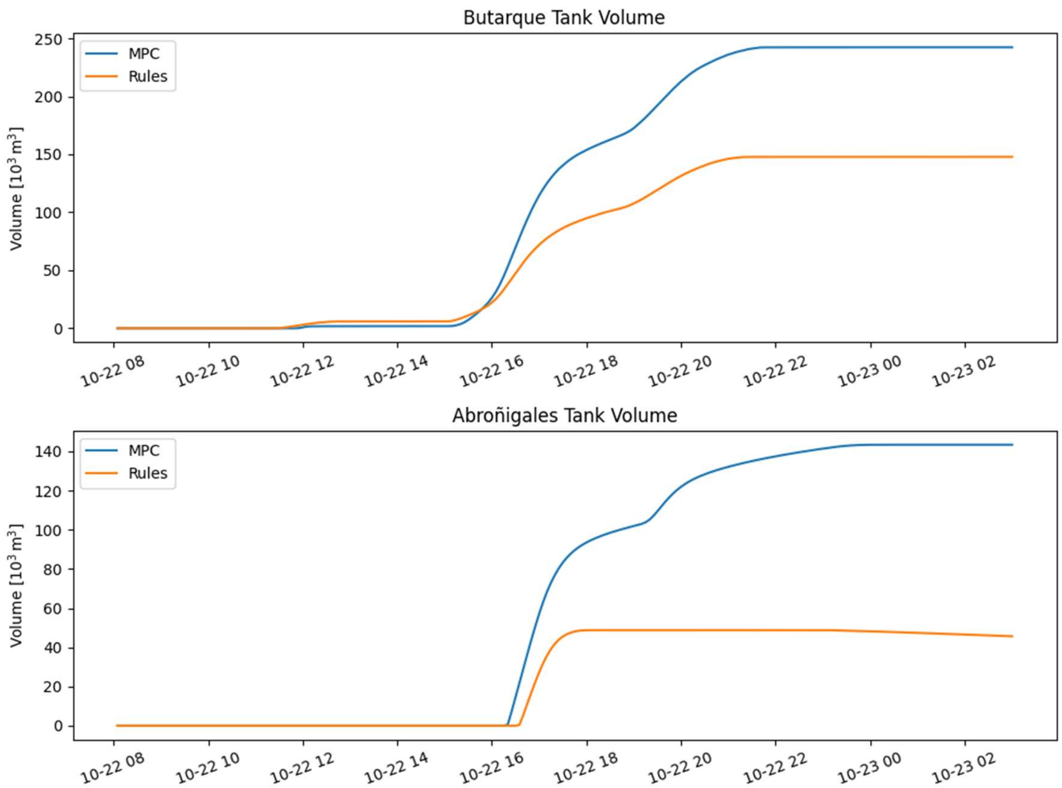

Figure 30 Volume stored in detention tanks during rain event P0 obtained by the MPC controller and the current operation rule-based controller for the different rain events.

5.4.3 WWTP Usage

It is common that WWTPs work at full capacity during rain events due to the increased flowrates occurring in the network in those periods. Therefore, the difference in treated volume is not relevant between the two analysed controllers. The small difference reported in Table 8 can be explained by the different behaviour while choosing to route part of the flow to the corresponding storm water tank. Notice that, if water stored in the tanks at the end of the rain event is to be considered as eventually treated in WWTPs, the MPC controller would provide a big increase in this indicator. Figure 31 shows the influent time-series at each of the considered WWTPs.

	MPC Volume [$10^3 m^3$]	Rules Volume [$10^3 m^3$]	Difference [$10^3 m^3$]
Butarque WWTP	179	212	-33
Sur WWTP	323	286	37
Total	503	498	5

Table 8 Total WWTP influent volumes for rain event P0 obtained by the MPC controller and the current operation rule-based controller for the different rain events.

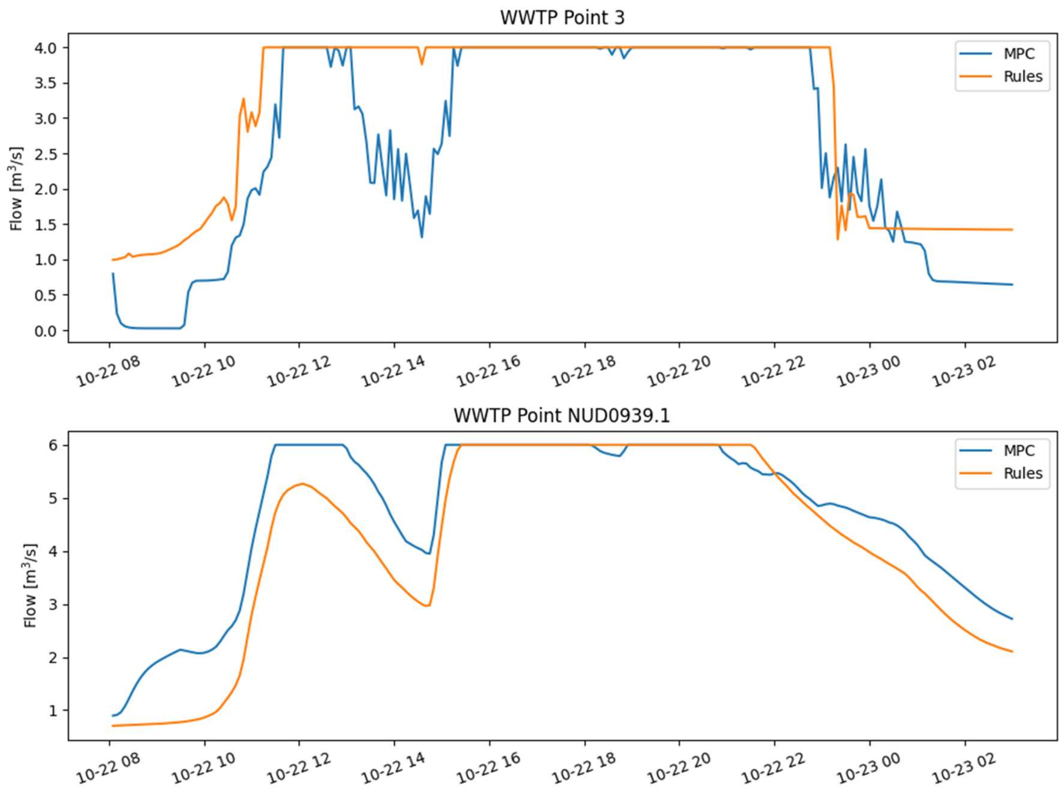

Figure 31 WWTP influents obtained by the MPC controller and the current operation rule-based controller for the different rain events.

5.4.4 Actuator Setpoints

For the MPC methodology to work properly it is required that the simplified model provides good approximations of the real system dynamics (here, virtual reality). To his end, besides the model equations, the input flow forecasts and the initial conditions, it is very important that the system actuators implement properly the setpoints computed by the simplified model. Only if these setpoints are accurately reproduced by the real system will the simplified model predictions become accurate and the whole MPC loop work as expected.

The simplified model does not make use of water levels or gate positions, but of flows only. Therefore, after a flow setpoint is computed by the OCPs a flow-setpoint function must be used to transform the desired flow into the corresponding actuator setting, in this case a gate opening. Figure 32 shows the set-points computed by the OCPs as the first time-step of the solution and the corresponding flows computed by the SWMM simulator. The computed gate positions result into flows tracking the setpoints very accurately.

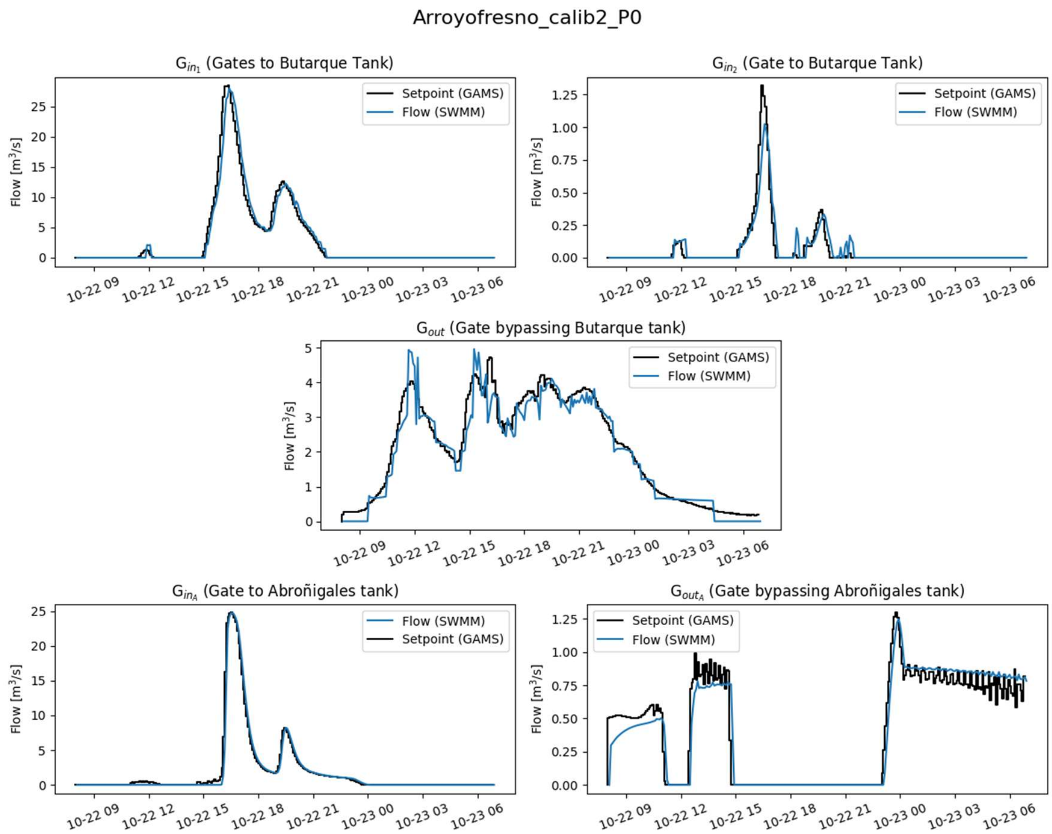

Figure 32 Flow set-points computed by the MPC controller and corresponding SWMM flows during rain event P0.

6 Conclusions and next steps

This deliverable describes the work carried out in sub-action "B.3-3: Virtual testing" (Action B.3 of LIFE RUBIES project) and the associated main findings. The main activity of this sub-action focuses on adapting the MPC controller considered in Madrid pilot site to the characteristics of the network and test its performance in comparison with the current operation, considering real rain scenarios and using the Madrid pilot detailed sewer model as a virtual reality. With this purpose, a software demonstrator has been developed (Chapter 2) in order to reproduce the real-time closed-loop interaction between the reality and the controller.

In Chapter 3 and 4, the MPC Controller methodology and the main developments needed to adapt the MPC Controller to Madrid pilot characteristics are described: mainly, development of the needed simplified model associated with the Madrid pilot network.

Finally, in Chapter 5, the results obtained comparing the MPC controller and the current operation performance considering real rain scenarios and using the software demonstrator is described. The results show the MPC controller can reduce CSO volumes in all scenarios by routing larger volumes to the storm tanks. Treated wastewater volumes are almost identical for both controllers since WWTPs work at maximum capacity during rain events. Tank volumes at the end of the events is to be considered as potentially treated water during a following dry weather period and would eventually be added to the WWTPs treated volume[2]. In this sense, there are two CSO points in which the MPC controller can reduce the CSO with respect to the current operation: both correspond to the CSO structures immediately downstream of the two detention tanks. The MPC controller is more flexible in adapting the gate positions to route larger volumes to the detention tanks thus reducing the downstream flowrate, preventing higher water levels and activation of CSO weirs.

The obtained results show a meaningful reduction of the CSO volumes regarding the default operation (Local Control rules) implemented in the hydraulic model provided by the operator, assuming tanks are empty at the beginning of the rain event. This may not be the case when two rain events occur in a short period of time and the second rain event starts when there are still some water volumes stored in the tanks. Consequently, the available tank volume for the second rain event is smaller, impacting negatively on the CSO reduction capacity of the controller. Additionally, in a real test, the CSO reductions could be smaller since the operator is able to adapt manually the Local Control Rules according to observed dynamics of the network, while in the virtual tests, the Local Control Rules are kept constant during all the rain scenarios.

As further steps, the emptying tank strategies during the rain event will be integrated to increase the capacity to store wastewater volumes and the MPC Controller will be tested using recent

---

[2] If a new rain event occurs before tanks are empty, the CSO reduction potential of the system will be constrained observing larger CSO volumes than the case all the tank volumes were available to store those flows than can not be treated in the WWTP.

rain events. Additionally, the MPC controller will be integrated into the AQDV Platform in order to enable real tests.

7 Appendices

7.1 KPI Comparison Details

7.1.1 CSO Volume

Rain Event	**MPC CSO Volume [10^3m^3]**	Rules CSO Volume [10^3m^3]	Absolute CSO Variation [10^3m^3]	Relative CSO Variation [%]
P0	278	438	-160	-36
P1	949	1022	-74	-7
P2	505	654	-149	-23
P3	380	583	-203	-35
P4	263	411	-148	-36
P5	258	422	-164	-39
P8	125	257	-132	-51
P9	312	522	-210	-40
P10	168	314	-146	-46
Total	3238	4623	-1385	-30

Table 9 CSO volumes and comparison for the MPC and the current Rule-based controllers for the 9 simulated rain events.

7.1.2 WWTP Volume

Rain Event	MPC WWTP Volume [10^3m^3]	Rules WWTP Volume [10^3m^3]	Absolute WWTP Variation [10^3m^3]	Relative WWTP Variation [%]
P0	503	498	5	1
P1	797	799	-2	0
P2	404	392	12	3
P3	1127	1147	-20	-2
P4	540	538	2	0
P5	337	333	4	1
P8	270	260	10	4
P9	560	570	-10	-2
P10	262	254	8	3
Total	4800	4791	9	0.2

Table 10 WWTP volumes and comparison for the MPC and the current Rule-based controllers for the 9 simulated rain events.

7.1.3 Tank Volume

Rain Event	MPC Tanks Volume [$10^3 m^3$]	Rules Tanks Volume [$10^3 m^3$]	Absolute Tanks Variation [$10^3 m^3$]	Relative Tanks Variation [%]
P0	386	193	192	99
P1	559	505	54	11
P2	559	416	143	34
P3	429	199	230	115
P4	432	253	179	70
P5	401	223	178	80
P8	265	151	114	75
P9	488	271	218	80
P10	344	199	145	73
Total	3863	2410	1453	60

Table 11 Final ta tank volumes and comparison for the MPC and the current Rule-based controllers for the 9 simulated rain events.

8 References

Camacho, E. F., Bordons, C. (2004). Model predictive control. ISBN 3-540-76241-8 Springer-Verlag Berlin Heidelberg New York

Puig, V., Cembrano, G., Romera, J., Quevedo, J., Aznar, B., Ramón, G., & Cabot, J. (2009). Predictive optimal control of sewer networks using CORAL tool: application to Riera Blanca catchment in Barcelona.